LAPPEENRANTA UNIVERSITY OF TECHNOLOGY

SCHOOL OF ENGINEERING SCIENCE

DEGREE PROGRAM IN CHEMICAL AND PROCESS ENGINEERING

Mehmet Emin Küçük

REMOVAL OF SULFATE AND PHOSPHATE BY ZN-AL LAYERED DOUBLE HYDROXIDES

MASTER'S THESIS

2017

Examiner: Professor Mika Sillanpää

Supervisors: Doctor of Science Eveliina Repo

Doctor of Science Varsha Srivastava

ABSTARCT

Lappeenranta University of Technology

Chemical and Process Engineering Department

Mehmet Emin Küçük

Removal of Sulfate and Phosphate by Zn-Al Layered Double Hydroxides

Lappeenranta 2017

77 pages, 29 figures, 10 tables and 1 appendice

Examiner: Professor Mika Sillanpää

Supervisors: Doctor of Science Eveliine Repo

Doctor of Science Varsha Srivastava

Keywords: adsorption, sulfate removal, phosphate removal, layered double hydroxides, water treatment

Sulfate and phosphate are irreplaceable nutrients for living mechanisms. If not present in excessive levels, these compounds are not toxic for humans. However, waters highly concentrated in terms of sulfate and phosphate cause extraordinary taste and odor in water. Sulfate is responsible for water hardness, gastrointestinal problems for humans and corrosion in metals. Excessive phosphate amount leads to eutrophication in water sources. Furthermore, phosphate is widely used as a fertilizer; therefore, removal and recovery studies of both nutrients have accelerated in last decades.

Zn-Al Layered Double Hydroxides (LDH) with different Zn-Al rates were synthesized and characterized, their sulfate (SO_4^{2-}) and phosphate (PO_4^{3-}) removal performances from aqueous solutions by adsorptive methods were investigated as a comparative study. The results showed that the synthesized adsorbent exhibits outstanding removal performances for both sulfate (>80%) and phosphate (>90%). High nutrient uptake was observed in a wide pH range.

The kinetic data followed the pseudo-second-order model for both compounds suggesting that the adsorption processes were controlled by the surface reactions. The Sips isotherm model was found to be the best model to define the adsorption equilibrium conditions. Moreover, the slight positive effect of temperature increase was observed which confirmed that the adsorption process was endothermic. For regeneration of the adsorbents NaCl solution was found to be suitable for the regeneration cycle.

ACKNOWLEDGEMENTS

The research work of this thesis was carried out at Laboratory of Green Chemistry, Lappeenranta University of Technology, Mikkeli between September 2016 and February 2017.

First, I would like to mention my gratefulness to my examiner Professor Mika Sillanpää for giving me the opportunity to work in this project under his leadership. Due to their considerable help and encouragement, I am thankful to my supervisors D.Sc. Eveliina Repo and D.Sc. Varsha Srivastava. In addition, special thanks to the Laboratory of Green Chemistry staff because of their welcoming and positive attitude during my working period.

The greatest thanks go to my family Ayfer Küçük, Mehmet Küçük, Pelin Doğan and Okan Doğan due to their enormous support throughout my both academic and personal life. I believe that I am blessed with my family as they have been always willing and ready to help me without any hesitation. Therefore, I attribute this thesis to my dear family. Finally, I would like to express my gratitude to all my friends and in particular to Ezgi Sönmez Turan who has given me the strength and motivation to accomplish this thesis.

Lappeenranta, July 2017

Mehmet Emin Küçük

TABLE OF CONTENTS

LIST OF SYMBOLS AND ABBREVIATIONS

A	Surface area	cm^2
C_b	Weber morris constant related to the boundary layer	$mg/gmin^{-0.5}$
C_e	Equilibrium concentration	mg/L
C_i	Initial concentration	mg/L
G	Standard gibbs free energy	J/mol
H	Enthalpy	J/mol
K_{ads}	Adsorption equilibrium constant	mg/L
K_F	Freundlich isotherm constant	-
K_L	Langmuir isotherm constant	-
K_S	Sips isotherm constant	-
K_T	Temkin isotherm constant	-
P	Pressure	Pa
R	Ideal gas constant	J/molK
R^2	Coefficient of determination	-
S	Entropy	J/molK
V	Solution volume	L or mL
T	Temperature	ºC or K
b_T	Temkin constant	-
k_1	Pseudo-first-order model rate constant	min^{-1}

k_2	Pseudo-second-order model rate constant	g/mg min
m	Adsorbent weight	mg
n	Heterogeneity factor	-
q_e	Equilibrium adsorption capacity	mg/g
q_t	Adsorption capacity as a function of time	mg/g
t	Time	min
α	Elovich initial sorption rate	g/gmin
β	Elovich adsorption constant	g/g

1. INTRODUCTION

Due to continuous production activities of the industries and population growth, the global pollution problem is aggravating. Chemical industry has an important role in global pollution due to the enormous waste streams produced and it is responsible for soil, water and air pollution. Heavy metals, aliphatic and aromatic organic substances, volatile organic compounds and nutrients can be given as the major pollutants caused by chemical industries. As being nutrients, excessive amount of sulfate and phosphate in water sources might cause pollution problems as well as they deteriorate the quality of drinking water. Therefore, removal of these two compounds have attracted a considerable research interest in the last decades (Huang et al., 2017).

Most of the natural water sources contains a certain amount of sulfate ion and it occurs when several sulfate minerals dissolve in water and when sulfate containing industrial effluents are discharged. Acidic sulfate wastewater is introduced from electroplating, steel pickling, flue gas desulfurization, textile, landfill, mining and nonferrous smelting processes (Sadik et al., 2015).

Sulfate does not pose a vital risk on human health unless it is very concentrated in the water. Nevertheless, the low amount of sulfate in drinking water leads to unaccustomed odor and taste, while catharsis, dehydration, gastrointestinal problems might arise at highly concentrated waters in terms of sulfate (Namasivayam and Sangeetha, 2008; Sepehr et al., 2014). In addition, high concentrations of sulfate can cause corrosion problems of reinforced steel, might impede scaling of the equipment and can increase the formation risk of toxic and highly corrosive hydrogen sulfide (H_2S), particularly in sewer systems. Sulfate is considered as a major contaminant in waters when it exceeds 250 mg/L (Sadeghalvad et al., 2016; Liu et al., 2014). Maximum sulfate concentration has been limited in many countries for both industrial and drinking water in order to avoid pollution problems and protect the equipment maintenance and human health (Dou et al., 2017; Runtti et al., 2016; Silva, Lima and Leao, 2012).

Phosphate is an indispensable nutrient for all life forms. The productivity of the ecosystems in marine environments are limited by phosphate, it has a vital impact in DNA/RNA molecules and it plays a very important role in agriculture as it is used as fertilizer. It usually occurs in wastewaters in forms of organic phosphates, inorganic phosphates, polyphosphates and oligo

phosphates (Novillo et al., 2014). Despite her irreplaceable role above mentioned, excess amount of phosphate which is produced as waste from industrial, agricultural and household activities leads to eutrophication of lakes, sea, oceans, rivers and lagoons. Thereby, water eutrophication has become a global issue in recent years. It is stated that the total phosphorus contaminant level in water resources is in the vicinity of 0.01 – 0.1 mg/L. However, the requirements have already been exceeded as they are between 0.005 – 0.05 mg/L (Huang et al., 2017). Consequently, phosphate recovery and removal studies have gained a drastic importance in last decades as it provides the opportunity to water protection from pollution as well as sustainable and renewable recovery and utilization (Yu, 2015).

Layered double hydroxides (LDH) are hydrotalcite like materials with brucite-like structure ($Mg(OH)_2$) is present where magnesium ions occupy the octahedral sites in the material. Hydrotalcites are the one of the oldest LDH groups where trivalent ions like Al^{3+} take the place of divalent cations (Mg^{2+}). The positive charge in the LDH layers are balanced with anions. These anions can be either intercalated between the layers or to the surface of the material. Due to this structure, LDHs exhibit very good anion exchange capacity; however, the low cation exchange capacity is a drawback of these clay minerals (Theiss, 2012, 3-4; Theiss et al., 2016).

2. THEORITICAL BACKGROUND

2.1 Sulfate removal technologies

Sulfate removal from aqueous solutions can be achieved by biological treatment (Kijjanapanich et al., 2013), chemical precipitation (Nurmi et al., 2010; Silva, Codorin and Rubio, 2010), crystallization (Tait et al., 2009), electrodialysis (Fu et al., 2009), nano-filtration (Van der Bruggen and Vandecasteele, 2003), ion exchange (Apell and Boyer, 2010) adsorption (Sepehr et al., 2014) and reverse osmosis (Bódalo et al., 2004), distillation and evaporation (Sepehr et al., 2014). Production of high sludge amount volume and the difficulty of pH adjustment of the treated waters are the drawbacks of the precipitation method. With addition of barium or calcium salts, high removal rates can be achieved in short times; however, the high cost and toxicity of barium salts force engineers to develop alternative methods. Moreover, this method is effective with highly concentrated waters which brings the difficulty of disposal of solids and appropriate separation systems. Lime precipitation is more propitious in terms of price and toxicity but its efficiency is limited due to high calcium sulfate solubility (Benatti et al., 2009; Runtti et al., 2016; Silva et al., 2012). Despite their outstanding sulfate removal performance, high operational costs are stipulated by ion exchange, electrodialysis, reverse osmosis and membrane filtration systems. In addition, membrane fouling is another risk to be taken into consideration (Júnior, Gurgel and Gil, 2010; Sepehr et al., 2014). Biological treatment is feasible for low or moderate sulfate loaded wastewater (Qian et al., 2015; Silva et al, 2012). Furthermore, its application is constrained by produced hydrogen sulfur, lack of organics in the solution, metal ions in the water (Mothe et al., 2017; Runtti et al., 2016).

Adsorption on the other hand, have been commonly applied method due to its low-cost and high efficiency (Dou et al., 2017; Liu et al., 2014; Madzivire et al., 2010; Namasivayam and Sangeetha, 2008; Runtti et al., 2017; Sadik et al., 2015; Sepehr et al., 2014)

2.2 Phosphate removal technologies

Chemical precipitation is an efficient method for high phosphate concentration; however, it requires an elaborative process control as well as an accurate dosing requirement (Tillotson, 2006). Biological treatment is also commonly applied considering their relatively high removal

rates; however, they require complex and expensive cycling systems to remove the aerobic effluent (Hesselmann et al., 2000). High cost or inadequate removal performances are significant drawbacks of reverse osmosis and electrodialysis methods (Rodrigues and da Silva, 2009). Although crystallization has been widely utilized and has given promising results, crystal size distribution control is still an important obstacle (Qiu et al., 2017). Ultrasonic technology has become a considerable technology for this purpose and it was assisted by cavitation effect, high temperature pyrolysis, advanced oxidation processes (AOP) (Gordon, Kazemian and Rohani, 2012; Patist and Bates, 2008).

Adsorption is one of the most commonly applied methods for treatment of phosphate contaminated water due to its low sludge production, operation ease and rapid adsorption rate, superior selectivity, and more rapid regeneration process (Yang et al., 2014). The annual cost of chemical precipitation process has been calculated to be 10% lower than adsorption process. However, by means of adsorption, it is possible to reduce phosphate level more compared to precipitation (Huang et al, 2017; Jiang et al., 2004).

2.3 Basic concepts of adsorption

The term sorption has been widely used in several applications such as purification and separation in different scales. The word sorption might refer to both adsorption and absorption, which are two different processes. Absorption is the process of removing a part of a gas compound by means of a liquid in which the gas is dissolved, while adsorption refers to the accumulation of the obtained gas or liquid compound on the surface of the solid and remaining attached to it. In adsorption process, taken and accumulated ion is called adsorbate where adsorbent refers to the solid on which the adsorbate is attached. When saturation point is exceeded with maximum amount of adsorbate accumulated on the surface, the adsorbent needs to be regenerated. For this purpose, bound gas or liquid is removed from the surface and released into a medium; thereby, the adsorbent is restored for multiple operations (Hassan et al., 2015, Lefebvre and Tezel, 2017).

Adsorption process is a surface phenomenon where adsorbent surface area, pore volume, temperature, concentration, solution pH, pressure, nature of the adsorbent and adsorbate, and adsorbent dosage play a vital role to determine the performance of the adsorbent. Adsorption

process can be investigated under two titles: physiosorption where the adsorbate and molecules are attached to each other with weak Van der Waals forces. Chemical composition of adsorption pair remains the same here unlike chemisorption where different chemical structures occur due to electron share between the adsorption pair (Hassan and Mohamad, 2012; Hassan et al., 2015). A more detailed description and differences of the parameters in these sorption phenomena are provided in Table 1.

Table 1. Properties of physiosorption and chemisorption (Repo, 2011; Jafari 2016)

	Physiosorption	Chemisorption
Sorbate structure	Monolayer	Monolayer, multilayer
Adsorption kinetics	Fast	Slow
Desorption	Reversible	Mostly irreversible
Adsorption enthalpy, kJ/mol	5-40	40-800
Temperature effect	Low temperatures required	Occurs at wide temperature range

Over the last decade, adsorption has been widely used in different application areas such as: petrochemical industry, separation of gases, wastewater treatment and heterogeneous catalysis processes (Czelej, Cwieka and Kurzydlowski, 2016). Taking its significant contribution to chemical processes into consideration, particularly adsorption equilibrium modeling studies have been increased and great achievements have been gained in terms of process optimization.

2.4 Adsorbents

Adsorbents are the solid materials whose surfaces are used for the accumulation of the desired compounds and they play important roles in the extent of adsorption processes. Activated carbon, silica gel, MCM-41, MCM-48, activated alumina, zeolites and molecular sieves, carbon nanotubes, pillared clays, polymeric resins have been widely applied in gas – bulk separation, gas purification, liquid – bulk separation and liquid purification due to their superior characteristics (Yang, 2003).

The performance of an adsorbent is dependent on the solid's performance in equilibria and kinetics. High adsorption capacity is an asset; however, if the contact time is too long, the efficiency of the adsorbent reduces. Same way, a rapid adsorption with low capacity is also undesired. Therefore, optimum solids fulfilling these criteria should be chosen in order to meet these needs (Do, 2008).

i. The adsorbent should comprise high surface area or micropore volume.
ii. The adsorbent must have large pore network for molecule transformation into the inner layers.

IUPAC classified the pores and the structure of the sorbent according to the pore diameter as follows (Do, 2008):

Micropores	$d < 2$ nm
Mesopores	$2 \text{ nm} < d < 50$ nm
Macropores	$d > 50$ nm

A favorable adsorbent is also expected to exhibit following characteristics: high energy density, high energy efficiency, high adsorption capacity, high adsorbent-adsorbate affinity, satisfactory potential for regeneration, ease of operation, cost-efficiency, low desorption temperature, low toxicity and low environmental impacts (Lefebvre and Tezel, 2017, Tholiso et al., 2017).

In this thesis, adsorption performances of layered double hydroxides (LDH) have been investigated for sulfate and phosphate; the effect of adsorption parameters has been determined and adsorption process has been optimized.

2.5 Layered double hydroxides (LDH)

Layered Double Hydroxides (LDH) also known as anionic clays are nanostructured materials containing multiple intercalating exchangeable anionic metal layers represented as $[M^{2+}_{(1-x)} M^{3+}_{(x)} (OH)_2]^x(A^{n-})_{x/n}.mH_2O$. M^{2+} and M^{3+} denote the divalent and trivalent metallic cations such as Mg^{2+}, Cr^{2+}, Ca^{2+}, Fe^{2+}, Mn^{2+} and Co^{2+}; Al^{3+}, Co^{3+}, Fe^{3+}, Cr^{3+} and Mn^{3+} that are utilized in the synthesis of the LDH. A^{n-} represents the replaceable interlayer ions such as Cl^-, NO^{3-}, CO_3^{2-}. X values in the formula vary between 0.20 and 0.33 and the molar ratio of M^{2+} and M^{3+}

vary between 2.0 and 4.0 (Daud et al., 2016; Mallakpour and Hatami, 2017; Sajid and Basheer, 2016; Zubair et al., 2017).

The alignment of brucite-like layers stacking determines the configuration of the LDH molecule. There are two or three layers per a unit cell which form a hexagonal symmetry or rhombohedral symmetry, respectively. In addition, less symmetric alignments can be observed. The interlayer of LDHs accommodate both water molecules and interlayer anions. There is a complex hydrogen bonds between the layer hydroxyl groups, water molecules and anions causing an extremely structured LDH (Duan and Evans, 2006, pp. 11). The structure of a LDH molecule is demonstrated in Figure 1.

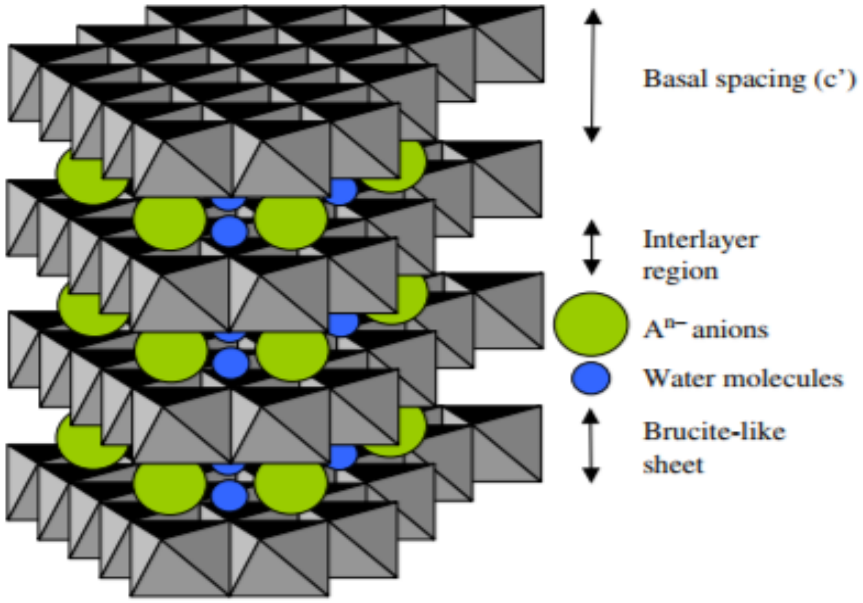

Figure 1. Schematic representation of LDH structure (Goh et al., 2008)

An important factor affecting the properties of LDH molecule is its rigidity. If compared, LDH is much more rigid than graphite and metal dichalcogenides while they are less rigid than vermiculite. LDHs are considered to have relatively rigid layers where strong forces are applied towards the interlayer molecules (Duan and Evans, 2006, pp. 12).

LDH molecules exhibit an outstanding capacity for removal of organics and inorganics due to their weak interlayer bonding band. They have very large surface area and good thermal stability. In addition, their anion exchange capability is almost as good as commercial organic

anion exchangers (Bish 1980; Cavani et al., 1991; Vaccari, 1998; Das et al., 2004; Goh et al., 2008).

LDH materials have been applied in several purposes such as supercapacitors (Cai et al., 2015), in catalysis (Li et al., 2014; Tichit and Coq, 2003;), in drug delivery (Ladewig, Xu and Lu, 2009), in fuel cells (Lee et al., 2005), in electrochemical sensors (Du et al 2008) and biosensors (Chen et al., 2008; Shan, Cosnier and Mousty, 2003), flame retardants (Matusinovic and Wilkie, 2012) and as adsorbents in water treatment (Das et al., 2006; Goh et al., 2008). Due to their high surface area, non-toxicity, anionic exchange ability, water resistant structure and high porosity, their application in water treatment has gained considerable importance (Sajid and Basheer, 2016, Zubair et al., 2017).

Several pollutants, nutrients and valuable components have been separated from water by using LDH adsorbents. A brief summary can be given as following: chromium (Jaiswal et al., 2015, Zhang et al., 2017), borate (Qiu and Wong, 2017), congo red (Long et al., 2016), methyl orange (Chen et al., 2016), nitrate (Halajnia et al., 2013), boron (Gao et al., 2017), iodide (Theiss et al., 2016), copper, lead and cadmium (Rojas, 2014), arsenic (Hong et al., 2014), phenol and 4-nitrophenol (Chen et al., 2009), nickel (Chen et al., 2016), fluoride (Kameda et al., 2015), yttrium, cerium and lanthanum (Iftekhar et al., 2017), 2,5-dihydroxybenzoic acid (Tang et al., 2015), antimony (Cao et al., 2017), manganese (Bakr et al., 2016), zinc, mercury and silver (Ma et al., 2016) and herbicides (Cardoso and Valim, 2006).

LDH synthesis methods can be listed as follows: co-precipitation method, ion-exchange process, reconstruction (memory effect) method, alkoxide and alkoxide-free sol-gel methods, preparation using solid precursors, preparation using organic neutralizers, stabilizers or metal organic ligands and the urea method (Chubar et al., 2017; Duan and Evans, 2006, pp.92).

The oldest and most popular method is co-precipitation method where aqueous solutions of M^{2+} and M^{3+} or their mixtures and caustic compounds with pH of 9-10 are applied. As metal sources, metal nitrate and chloride solutions are applied due to LDH's low selectivity for these ions. The two solutions are mixed, and the pH is adjusted while with vigorous stirring at high temperatures. The slurry obtained is filtered, washed, dried and homogenized (Duan and Evans, 2006, pp.92; Theiss et al., 2016).

Different ratios of the metal compounds generate LDH compounds with different properties. For some compounds, a wide range of M^{2+}/M^{3+} can be applied such as Zn/Al-CO_3 while narrow range of ratio is acceptable for some types (Duan and Evans, 2006, pp.92).

Calcination is an important additional step for enhancing the adsorption capability of the sorbents. When calcined, following behaviors are obtained in the structure: increase in the porosity due to high temperature, increase in the surface area and less carbonate anions in the interlayer (Goh et al., 2008).

It is important to mention various mechanisms facilitating the adsorption of these anions. When calcined, layered double hydroxides procure a remarkable ability called memory effect in aqueous medium. In case of memory effect, the inner reaction of adsorbent and the adsorbate is facilitated and the surface defects are enhanced. This phenomenon can be considered as a reconstruction in the structure occurring at a certain high temperature leading a thermal decomposition where the water molecules and interlayer anions are destroyed and an oxides-mixture is obtained. It is possible to introduce numerous species into the interlayer of LDH molecule such as organic, inorganic and bimolecular ions. In addition, the effect of ion exchange, surface complexation and co-precipitation must be considered (Otgonjargal et al., 2017).

To sum up, the removal efficiency of the ions depends on the concentration of the ions, metals used for LDH synthesis, molar ratio of divalent and trivalent cations, synthesis method, calcination and adequacy of solid crystallinity (Halajnia et al., 2013).

2.5.1 Literature review for layered double hydroxides application for phosphate and sulfate removal

LDH type adsorbents form an important application area in phosphate and sulfate removal with adsorptive methods. Table 2 demonstrates the list of these two nutrients investigated for their adsorption characteristics with several LDH materials.

Table 2. Literature review for sulfate and phosphate removal with LDH

Nutrient	LDH Type	Maximum adsorption capacity (mg/g)	Reference
Sulfate	Mg/Al LDH	255.8	Sepehr et al., 2014
Sulfate	Mg/Fe LDH	68.0	Liu et al., 2014
Sulfate	Mg/Al, Ni/Fe, Ni/Al, Mg/Fe Calcined LDH	17.99	Sadeghalvad et al., 2016
Sulfate	Mg/Al LDH	840.0	Sadik et al., 2015
Sulfate	Mg/Al LDH	12.48	
Phosphate	Mg/Al LDH	26.6	Halajnia et al., 2013
			Halajnia et al., 2013
Phosphate	Calcined Mg/Mn LDH	7.3	Chitrakar et al., 2005
Phosphate	Pyromellitic Acid Intercalated Zn/Al LDH	76.0	Yu et al., 2015
Phosphate	Mg/Al, Zn/Al, Ni/Al, Co/Al, Mg/Fe, Zn/Fe, Ni/Fe and Co/Fe	44.0	Das et al., 2006
Phosphate	Zn/Al LDH	68.4	Yang et al., 2014
Phosphate	Biochar with Mg/Al&Mg/Fe LDH	58.1	Wan et al., 2016
Phosphate	Zn/Al LDH	232.0	Zhou et al., 2011
Phosphate	Mg/Al LDH	71.2	Novillo et al., 2014
Phosphate	Mg_2/Al LDH	5.82	Zhan et al., 2016
Phosphate	Mg/Fe/Cl LDH	30.0	Ashekuzzaman and Jiang, 2017
Phosphate	Fe_3O_4/MgAl-NO_3 LDH	33.4	Koilraj and Sasaki, 2016

3. ADSORPTION PHENOMENON

3. 1 Isotherm studies

The relationship between the adsorbate in the liquid phase and the adsorbate adsorbed onto the adsorbent on constant temperature is illustrated with adsorption isotherms. An adsorption isotherm gives an information regarding to the process as the adsorption capacity and the isotherm type is provided. Today, four types of adsorption isotherms are commonly applied to reveal the equilibria of the processes: S-type, L-type, C-type and L-type isotherms are demonstrated below in Figure 2 (Repo, 2011, pp.26-27).

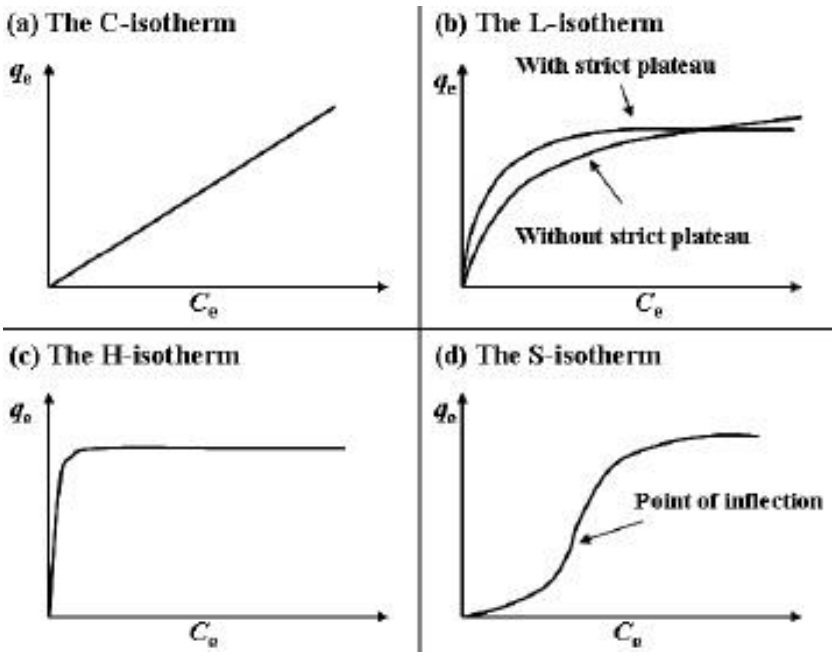

Figure 2. Adsorption isotherm shapes (Repo, 2011, pp.27)

Among these types, in C-type of isotherm, there is a constant ratio between the amount adsorbed and the ions to be adsorbed within the solution and the adsorption sites are unlimited. However, the acquisition of this type of data is possible only for a small number of phenomena in presence of low concentrations. L-type isotherm suggests the limit of the phenomena and once this limit is exceeded, the process decelerates. As being a special version of L-type, H-type isotherm proposes a high affinity between the adsorbent and the ion. S-type isotherm is observed less often than the other shapes and it shows that low adsorption affinity occurs in low concentrations

and the inflection point counteracts the competition between the ions and enhances the adsorption (Liubov, 2016, pp.28; Repo, 2011, pp.27,).

Langmuir isotherm model

The Langmuir adsorption isotherm was developed in order to understand the efficiency of the adsorbents. It is applied when a gas-solid or gas-liquid adsorption phenomenon takes place within a homogeneous system. It assumes that the adsorption takes place in adsorbent's homogeneous adsorption sites and all these sites have uniform energy levels. The equation 3.1shows the Langmuir Isotherm Model:

$$qe = \frac{q_m K_L C_e}{1 + KC_e} \qquad \text{(Equation 3.1)}$$

Where C_e Adsorbate concentration at equilibrium, (mg/L)

q_e the amount of adsorbate per unit mass, (mg/g)

q_m Maximum adsorption capacity, (mg/g)

K_L Affinity constant, (L/mg)

Although, it is used very commonly due to its simplicity, this model can be too simple to describe the mechanism where surface heterogeneity and non-uniform structure is involved. Therefore, other models have also found application areas in adsorption modeling.

Freundlich isotherm model

In this empirical model, surface heterogeneity and energy difference within the sites are also taken into account. The Freundlich model is commonly applied for heterogeneous adsorption and chemisorption processes, organics adsorption onto activated carbon and heterogeneous gas phase systems. However, it has a limitation from thermodynamic point of view as it cannot approach Henry's Law at low concentrations. The Freundlich model is shown in Equation 3.2 (Kinniburgh, 1986; Repo, 2011).

$$q_e = (K_F C_e)^{1/n} \qquad \text{(Equation 3.2)}$$

Where, K_f is equilibrium binding constant, L/mg

n is heterogeneity factor

As expected, when n approaches to unity, the adsorption becomes more linear. When value n is getting 10 times larger than unity, the isotherm approaches irreversible isotherm where the pressure or concentration must drastically decrease before the adsorbate molecules are desorbed from the solid's surface (Do, 2008).

Temkin isotherm model

In the Temkin Isotherm, adsorbent-adsorbate interactions are considered by using a factor. The model assumes that the increase in coverage will decrease the heat of adsorption linearly. While doing that, very high and low concentrations are ignored. The model equation can be given as follows (Foo and Hameed, 2010):

$$q_e = \frac{RT}{b_T} \ln(K_T C_e) \qquad \text{(Equation 3.3)}$$

Where R Ideal gas constant

RT/b_T adsorption heat (J/mg)

K_T equilibrium binding constant (L/mg)

Same as the Freundlich model, it has neither correct Henry`s law limit nor finite saturation limit. Therefore, its application is limited in low and high concentration or pressure (Do, 2008).

Sips (Three-Parameter) isotherm model

As being a combination of Langmuir and Freundlich Isotherm models, the Sips isotherm is also named as Langmuir-Freundlich Model (Hokkanen et al. 2014) and can be illustrated as follows:

$$q_e = \frac{q_m (K_s C_e)^n}{1 + (K_s C_e)^n} \qquad \text{(Equation 3.4)}$$

Where, n heterogeneity factor

K_s Sips isotherm affinity constant (L/mg)

This model provides better accuracy for heterogeneous adsorption processes then the other two models. In addition, it eliminates the limitation of Freundlich model to explain at low surface coverage and for the saturation of the adsorbed phase (Jafari, 2016). As seen, when *n* equals to 1, the equation becomes Langmuir model and can be used for homogeneous adsorption studies. At low concentrations, the model approaches to Freundlich model which means that it is a heterogeneous adsorbent, while Langmuir model is approached at high concentrations (Hokkanen et al. 2014).

Toth isotherm model

Sips isotherm removes the limit at high concentration of Freundlich model; however, it does not give accurate results in low pressure ranges. In order to address this challenge, Toth Isotherm model has been developed and widely applied. Being a three-parameter system like Sips model, Toth equation can define many adsorption systems with sub-monolayer and it can be shown as follows:

$$C_\mu = \frac{C_{\mu s}}{[1+(bP)^t]^{1/t}} \qquad \text{(Equation 3.5)}$$

Where, *t* and *b* are specific adsorbent-adsorbate parameters.

Langmuir equation is obtained when *t*=1; therefore, *t* is the parameter that determines the system heterogeneity. When the parameter *t* approaches to 1, it can be said that the system approaches to be more homogeneous (Do, 2008; Repo, 2011, pp.23).

3. 2 Kinetic studies

Adsorption kinetics provides the information to reveal the equilibrium time of the reaction. Therefore, kinetic studies are conducted as a function of time. By using obtained removal data at different time intervals, equilibrium time can easily be calculated for maximum adsorption capacity. Afterwards, the mechanism and order of reaction can be investigated by using kinetic models.

Adsorption process is accomplished in four stages until equilibrium conditions are reached:

i. The adsorbate is transferred from the bulk phase to the outer layer of the sorbent.
ii. Diffusion from the liquid film to the particles (external diffusion)
iii. Diffusion from the adsorbent particles to the surface (internal diffusion)
iv. There is either a chemical bond or a physical interaction between the adsorbate and the adsorbent which is called the surface reaction.

One of these above-mentioned steps takes place more slowly than the others and it is called the rate determining step as it determines the rate of the overall adsorption process. There are different models that have been developed to define the process and they assume the rate determining step as either one of the diffusion steps (diffusion models) or the surface reaction (reaction models). Major reaction models are Pseudo-first-order, pseudo-second-order and Elovich; while, Boyd's and Intra-particle models are the diffusion models (Liubov, 2016, pp.34; Repo, 2011, pp.34).

Pseudo-first order kinetic model (Lagergren Model)

The first-rate equation was developed to explain the kinetic process of sorption in solid/liquid systems by Lagergren in 1898 and it professes that number of effective adsorption sites has direct effect on the adsorption rate. In other words, with the increase of these sites, adsorption rate increases. The irreversible reaction applied to reveal the process is as follows:

$A + S \rightarrow AS$

Where, *A* adsorbate

S active sites of the adsorbent

There are 4 assumptions made in this model:

1. Adsorbate concentration is constant throughout the process.
2. The adsorption energy is not affected by surface coverage.
3. There is no interaction between the adsorbed ions.
4. Adsorption takes place on localized sites of the sorbent (Largitte and Pasquier, 2016).

The model can be shown as follows (Asuquo et al., 2017):

$$\frac{dq}{dt} = k_1(q_e - q) \qquad \text{(Equation 3.6)}$$

In the case of integration of this equation with initial and boundary conditions: q=o and q=q; t=0 and t=0, following equation is obtained:

$$\ln(q_e - q_t) = \ln q_e - k_1 t \qquad \text{(Equation 3.7)}$$

Where q_e adsorption capacity at equilibrium conditions, (mg/g)

q_t adsorption capacity at t (mg/g)

k_1 pseudo first order rate constant (1/min)

t time (min)

It is one of the most commonly applied models to reveal the sorption mechanism. However, for some cases, this linear equation may cause significant errors in the results as it is a linearized form of a non-linear equation and it is not accurate enough to determine the model parameters. For these cases, non-linear pseudo-first model is widely used and it is shown as follows (Asuquo et al., 2017):

$$q_t = q_e(1 - \exp(k_1 t)) \qquad \text{(Equation 3.8)}$$

$$ERRSQ = \sum_{i=1}^{n} (q_{t\exp} - q_{tcalc})^2 \qquad \text{(Equation 3.9)}$$

Where, q_e and k are given random values and by using error function, their actual values are calculated along with q_t.

Pseudo-second order kinetic model

The linear model was first developed by Azizan (Azizian, 2004) to explain the kinetics of sorption processes for low concentrations of adsorbate. However, according to Liu and Liu (Liu and Liu, 2008), the model was applicable for the first stages of adsorption. In addition, they

stated that low initial concentration is not needed for the implementation of this model (Repo, 2011, pp. 37). The Pseudo-second-order kinetic model can be demonstrated as follows:

$$\frac{dq}{dt} = k_2(q_e - q)^2 \qquad \text{(Equation 3.10)}$$

Where, k_2 is pseudo-second order rate constant, (g/mgmin)

Although it has been used for a long time to reveal the mechanism, like the linear-first order model, it has a major drawback in determination of model parameters. Therefore, a non-linear version of this model was developed and found to be more accurate after several modelling studies. There is one more advantage of this model: equilibrium capacity of the adsorbent can be calculated from the model instead of the experiment (Asuquo et al., 2017). If integrated with the boundary conditions q=0 and q=q; t=0 and t=0, following equation is obtained:

$$q_t = \frac{q_e{}^2 k_2 t}{1 + q_e k_2 t} \qquad \text{(Equation 3.11)}$$

$$ERRSQ = \sum_{i=1}^{n} (q_{t\exp} - q_{tcalc})^2 \qquad \text{(Equation 3.12)}$$

In Equation 3.12, q_e and k are given random values and by using error function, their actual values are calculated along with q_t.

Same assumptions are made for this model as the pseudo-first-order kinetic model.

Intra-particle diffusion kinetic model (Weber-Morris equation)

Diffusion models in mass transfer have found a wide application area in an attempt to study the sorption mechanisms. According to Weber and Morris, diffusion is constrained by one of these steps:

i) Diffusion of the adsorbate from the solution to the film of the particle
ii) Diffusion from the film to the particle (external diffusion)
iii) Diffusion from the film to the inside layers of the particle (internal diffusions)
iv) Adsorbate uptake onto the adsorbent

The model assumes that the adsorption process is occurring in a way that it is proportional with the root square of time (t^2) and the equation can be illustrated as follows (Asuquo et al., 2017, Ho, 2000, Qiu et al., 2009, Gürses et al., 2014, Alkan, Demirbaş and Doğan, 2007):

$$q_t = K_{id} t^{0.5} + C_b \qquad \text{(Equation 3.13)}$$

Where, C_b is the constant related to the thickness of the boundary layer ($mg/gmin^{-0.5}$)

Boyd's film diffusion model (liquid film diffusion model)

According to Boyd's Diffusion model, the outer layer of the adsorbent is the resistant step to diffusion and it can be shown as follows:

$$F = \frac{q_t}{q_e} = 1 - \frac{6}{\pi^2} \exp(-B_t) \qquad \text{(Equation 3.14)}$$

If B_t is left on the left side of the equation:

$$B_t = -0.4977 - \ln(1 - F) \qquad \text{(Equation 3.15)}$$

Above equation is obtained.

Where, B_t function of F and

F fractional attainment of equilibrium at different times

In order to find the rate determining step, B_t is plotted against t; pore diffusion controls the process if the plot is linear and passes through the origin. In case of obtaining a non-linear plot not passing through the origin, film diffusion or chemical reaction steps can be determining the steps (Ai et al., 2011, Loganathan et al., 2014, Hameed et al., 2008, Sharma and Das, 2013).

Elovich model

The model gives accurate results, particularly in case of heterogeneous chemisorption of gases. Additionally, soil adsorption and sorption kinetics have been revealed by this model. The general equation is as following:

$$q_t = \frac{1}{\beta}\ln(\alpha\beta) + \frac{1}{\beta}\ln(t) \qquad \text{(Equation 3.16)}$$

Where, α is elovich initial sorption rate, (g/gmin)

β is adsorption constant, (g/g)

When q_t versus *ln(t)* was plotted on a graph a linear relationship is anticipated to obtain and the intercept gives *(1/β)ln(αβ)*, while the slope gives *1/β*. It has been found out that the Elovich Equation is more accurate for short reaction times (Ahoroni and Ungarish, 1977; Inyang et al., 2016).

4. OBJECTIVE OF THE WORK

The purpose of the overall thesis was to inquire the sulfate and phosphate removal performance of Zn/Al layered double hydroxides (LDH). The main objectives of this research were:

1. Synthesis of Zn/Al and Zn/Fe LDH with different ratios of metals and study on the effect of calcination temperature on Zn/Al and Zn/Fe LDH properties.

2. To accomplish characterization of synthesized adsorbents.

3. To compare the removal efficiency of all prepared adsorbents for sulfate and phosphate.

4. To investigate the effect of various parameters on phosphate and sulfate adsorption.

5. To fit the experimental data to kinetics and isotherm models.

6. To reveal the adsorption mechanism for sulfate and phosphate adsorption.

7. To investigate the thermodynamic of the adsorption process and determination of the thermodynamic variables for phosphate and sulfate adsorption.

5. MATERIALS AND METHODS

5. 1 Synthesis of the adsorbents

In order to test their sulfate and phosphate removal properties, Zn/Fe and Zn/Al layered double hydroxides (LDH) were synthesized with different ratios. Afterwards, each adsorbent was calcined at different temperatures to find out the effect of the calcination temperature. The experiments were performed with Zn/Fe and Zn/Al adsorbents and the ones with different ratios and different calcination temperatures. Amongst them, the one exhibited best removal performance was chosen continued during the rest of the study.

ZnAl/LDH was prepared by co-precipitation method. First, 0.75 M $ZnCl_2$ and 0.75 M $AlCl_3.6H_2O$ were dissolved in 100 mL water, while 1M NaOH and 1M NaCl were mixed in 100 mL water in another beaker for the synthesis of ZnAl/LDH with a Zn/Al molar ratio of 1/1. For the preparation of ZnFe/LDH, $FeCl_2.4H_2O$ was used instead of $AlCl_3.6H_2O$. The adsorbents with different ratios were calculated based on this concentration range. NaOH/NaCl solution was dropwise added to the other solution which was vigorously being mixed at 70 ºC. 100 mL water was added in order to facilitate the mixing. Afterwards, solution pH was adjusted to 10 by using 1 M HCl to reach the supersaturation. The slurry was mixed for 24 hours at this temperature for enhancing the crystallinity of the solid, and the obtained precipitate subsequently washed until the pH was 7. Samples were dried in an oven at 50 ºC for 24 hours. Dried adsorbents were calcined at three different temperatures of 100 ºC, 200 ºC and 300 ºC. Finally, the particle distribution was homogenized by grinding and sieving.

5. 2 Characterization of the adsorbents

Fourier Transform Infrared Spectroscopy (FTIR, Bruker Vertex 70) and X-Ray Diffraction Spectroscopy (XRD, PANalytical X-ray diffractometer) analysis were carried out for identification of the functional groups in the structure and to detect the characteristic peaks in the LDH structure. The surface morphology of adsorbents was characterized by Scanning Electron Microscope (SEM). Brauner, Emmett and Teller surface area and pore volume of the adsorbents were measured with BET (BET, Tristar®II Plus) surface area analyzer. Zeta potential

measurement of the adsorbent Zn-AL/LDH was also carried out on order to reveal the resistance of the solid.

5. 3 Batch adsorption experiments

Applicability of LDH adsorbents for SO_4^{2-} and PO_4^{3-} removal was investigated using batch experiments. Zn/Al-LDH was used for SO_4^{2-} and PO_4^{3-} removal in order to obtain a comparative study for these two compounds. For each study, a certain amount of the compounds was dissolved in water and subsequently they were mixed with the adsorbents in centrifuge tubes. Agitation of all the solutions was obtained by a shaker with a rotation speed of 220 rpm at 25±2 ºC temperature.

For sulfate and phosphate removal studies, Zn-Al/LDH was applied to see the removal rate of these two compounds. Experiments for two ions were carried out separately. 1g/L of adsorbent dosage and 10 mL of solution volume were selected, after the dosage effect study was conducted. pH values between 2 and 8 were studied where 0.1 M NaOH and 0.1 M HCL were used for the pH adjustment purposes. Experiments with sulfate and phosphate solutions were carried out at four different temperatures from 25 ºC to 55 ºC for 10 different concentrations from 24 mg/L to 240 mg/L to reveal the effect of temperature.

After the required contact time was reached, solutions were separated from the adsorbents by filtration and subsequently analyzed with Inductively Coupled Plasma Optical Emission Spectrometry (ICP-OES) model iCAP 6000 (Thermo Electron Corporation, USA). The equilibrium adsorption capacity q_e (mg/g) was calculated with Equation 5.1.

$$q_e = \frac{(C_i - C_e)}{m} V \qquad \text{(Equation 5.1)}$$

Where, C_i the initial concentration of the solution (mg/L)

C_e equilibrium concentration of the solution (mg/L)

V solution volume (L) and

m weight of the adsorbent (mg)

5. 3. 1 Adsorption isotherms

For all the adsorption isotherm studies, solutions with different initial nutrient concentrations were used. In accordance with this purpose, optimum conditions were maintained in terms of pH, adsorbent dosage and contact time. A wide range of concentration was measured for sulfate and phosphate from 24 to 240 mg/L. The Langmuir, Freundlich, Sips and Temkin isotherm models were applied to reveal the adsorption mechanisms. Calculations for modelling were carried out using Microsoft Office Excel. Minimization of sum of the squares of the errors (ERRSQ) function was used as the criterion for this purpose.

5. 3. 2 Adsorption kinetics

As the aim of this study was to determine the effect of contact time, with 5 different concentrations (48 mg/L, 72 mg/L, 96 mg/L, 120 mg/L and 144 mg/L). The models were applied to 96 mg/L concentrated solutions as it was chosen the most favorable condition. For the modeling of the kinetics, the Pseudo-first-order, Pseudo-second-order, Intra-particle diffusion and Boyd's diffusion models were studied in this thesis.

5. 3. 3 Preliminary desorption and regeneration studies

For the regeneration study, 0.1 M and 0.5 M HCl, HNO_3, NaOH and NaCl solutions were used as desorption mediums. At first, the adsorbents were loaded by sulfate and phosphate ions with initial concentration of 96 mg/L and adsorbent dosage of 1g/L. Loaded adsorbents were contacted with these acidic, basic and neutral solutions for 5 hours. The concentration of desorbed ions was measured and the best desorbing medium was chosen among all and used for the regeneration cycles. The effect of desorbing medium on leaching of Zn, Al and Fe ions from adsorbent was also studied by measuring concentration of these ions in aliquot.

5. 4 Analysis of solutions

After the experiments and filtration, the solutions were analyzed by Inductively Coupled Plasma Optical Atomic Emission Spectrometry (ICP-OES). Sulfate and phosphate removal rates were obtained by using conversion factors for sulfur and phosphorus, respectively.

6. RESULTS AND DISCUSSION

6. 1 Characterization of the adsorbents

XRD analysis of the adsorbents

The XRD pattern of synthesized Zn-Al/LDH is demonstrated in Figure 3. Due to the fact that a cobalt cathode is applied in the XRD system, the results were converted into the traditional XRD patterns where copper is used and the converted patterns are shown. Most of the peaks are corroborative with the characteristics of a hexagonal structure. The peak (110) appearing at 62.9º confirms the formation of the layer structure (Li, Bai and Zhao, 2013). Peaks (012) and (018) are the characteristic diffraction peaks of a Zn-Al/LDH structure (Iftekhar et al., 2017). However, 2 characteristic peaks of LDH (003) and (006) corresponding the degrees around 10 and 20 theta were not obtained in the pattern. This absence can be explained with the collapse of LDH layered structure at 200 ºC and production of ZnO phase. It is assumed that with the decrease in calcination temperature, these characteristic peaks will appear again in the structure (Ahmed et al., 2012).

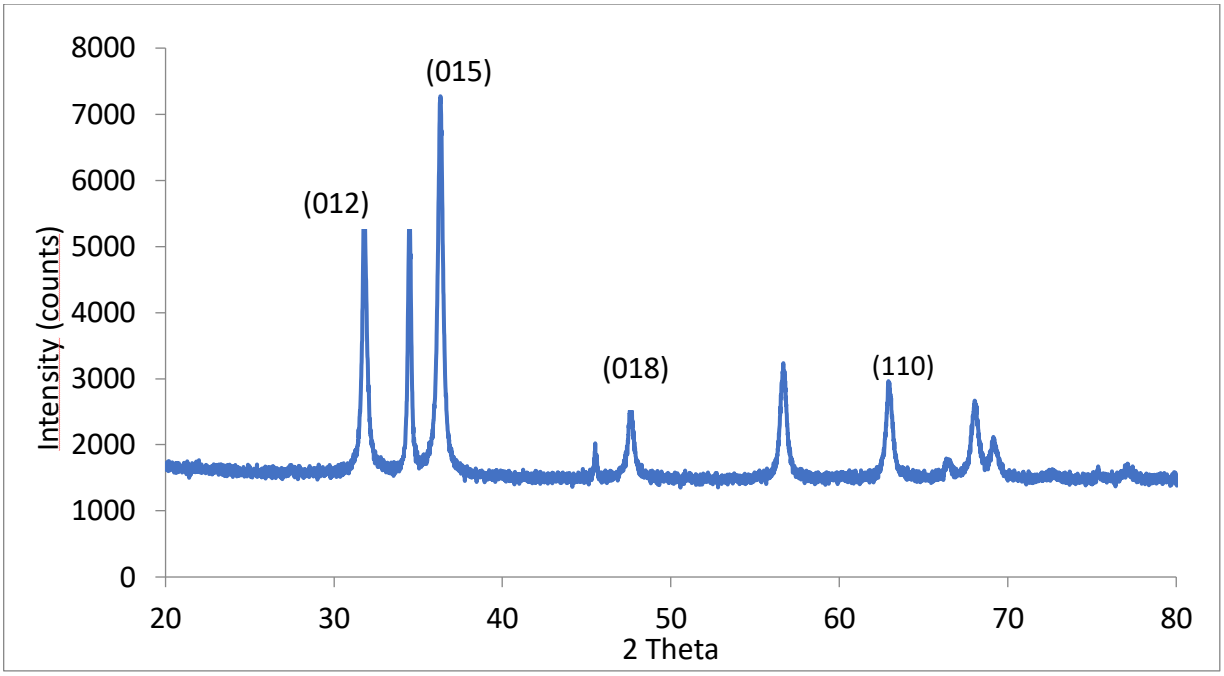

Figure 3. XRD patterns of the synthesized Zn-Al/LDH

FT-IR (Fourier transform infrared spectrometry) analysis

The hydroxyl groups and the interlayer anions are revealed with FT-IR; therefore, FT-IR plays in important role for the characterization of LDH. Figure 4 shows the FT-IR spectra of synthesized Zn-Al/LDH adsorbent. The intense band observed at 3522 cm^{-1} indicates the O-H stretching vibration of water molecular and hydroxyl groups, which confirms the brucite-like layers (Li, Bai and Zhao, 2013). The bands detected at 1614.5 cm^{-1} are attributed to O-H bending vibration and it occasionally is overlapped with any other peak (Yu et al., 2015). The bands below 1000 cm^{-1} are attributed to M-O stretching and M-OH bending vibrations in the brucite-like layer structure (Sepehr et al., 2014). The peaks at 804 $cm^{-1}$and 665 cm^{-1} are attributed to inorganic anions of NO_3^-(Goh et al., 2008).

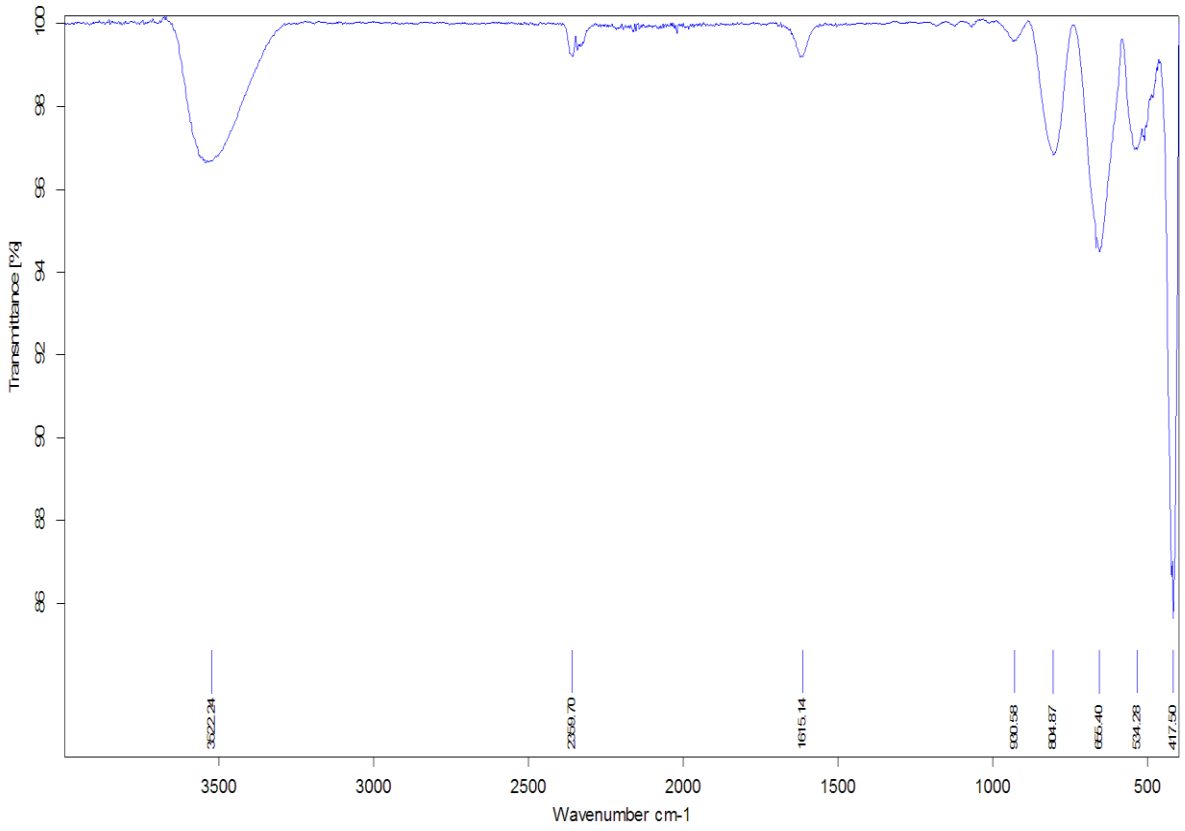

Figure 4. FTIR patterns of the Zn-Al/LDH

SEM analysis

In order to reveal the morphology of the samples, SEM analyses were carried out and the results are provided below. Figure 5, Figure 6 and Figure 7 demonstrate the SEM images of the raw Zn/Al LDH, sulfate-loaded and phosphate-loaded Zn/Al LDHs. All the images belong to the LDH sample that was calcined at 200ºC. The figures show the characteristic coral-like, crystalline structure of double hydroxides; however, due to calcination the structure was partly collapsed into small pieces with pores (Figure 5). This might have arisen from the release of the water in the structure. Numerous small plate-like structures gathered and formed the non-uniform, non-porous LDH structure in accordance with the previous studies (Ahgmed et al., 2012; Barahuie et al., 2014; Yin et al., 2010, Liu et a., 2015).

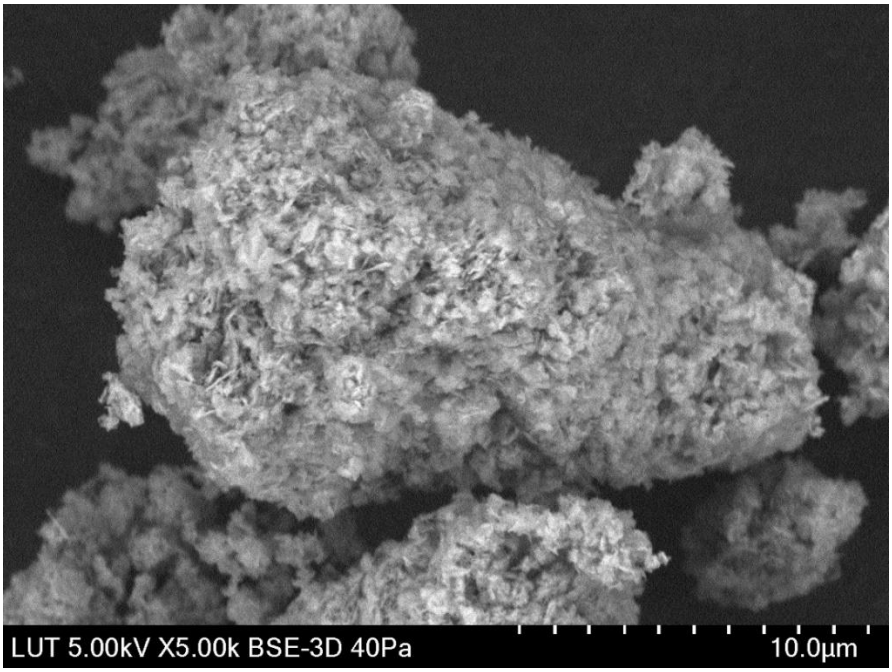

Figure 5. SEM image of the synthesized Zn/Al-LDH adsorbent

Figures 6 shows the solid structure after sulfate and phosphate uptake.

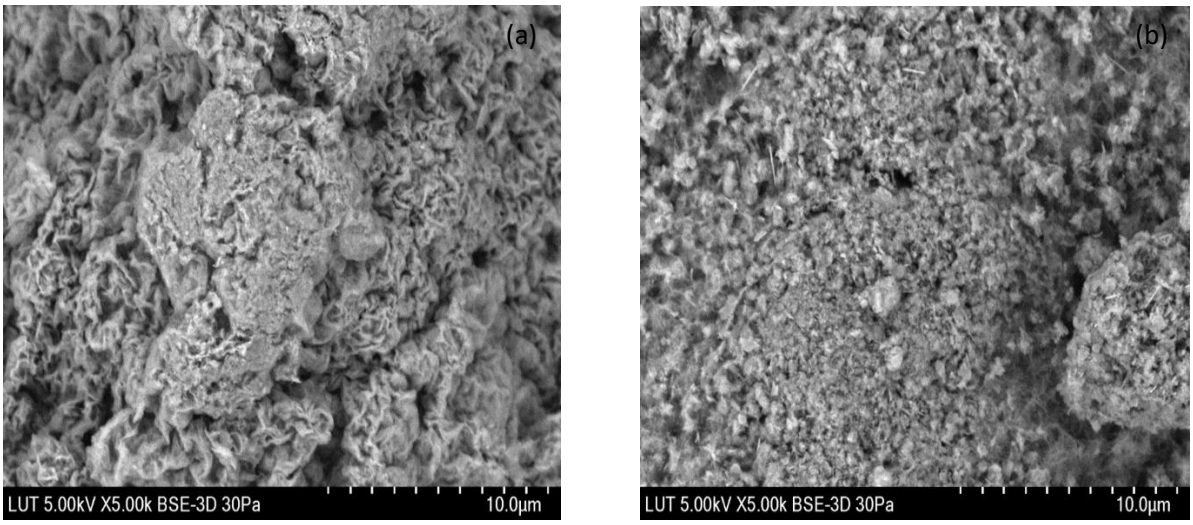

Figure 6. SEM image of Zn/Al LDH after sulfate (a) and phosphate uptake (b)

Figures 6 shows that after adsorption of sulfate and phosphate the LDH structure is more visible compared to Figure 5. The reason for this is so called memory effect, which occurs during rehydration and regeneration of interlayer anions (Goh et al., 2008).

EDS Mapping results

EDS mapping is another vital characterization method since it reveals the elements present in the solid and their distribution within the structure. Expected elements for an LDH molecule was found to be present in the structure such as C and O. In addition, the existence of Zn, Al and Cl was also proved in Figure 7 below.

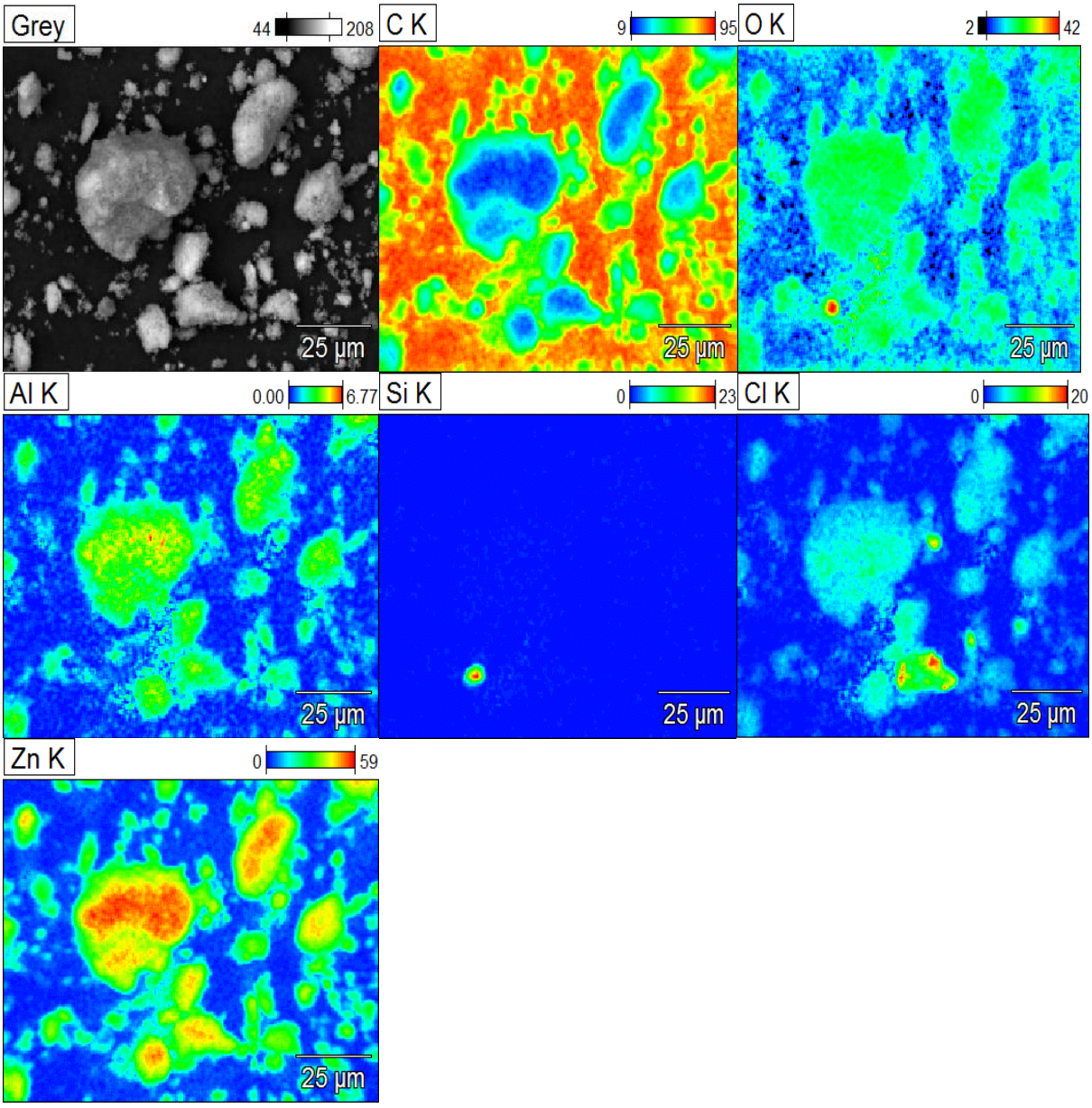

Figure 7. EDS mapping of elements in the synthesized ZnAl/LDH adsorbent

Sulfate and phosphate uptake can also be understood with these results as their amount significantly increased inside the pores of the solid as can be seen in Table 3 below.

Table 3. Amount of the elements in ZnAl/LDH before and after adsorption

Element	ZnAl/LDH	ZnAL/LDH after sulfate adsorption	ZnAL/LDH after phosphate adsorption
	Weight, %	Weight, %	Weight, %
C	8.65	19.1	9.7
O	22.33	29.2	26.8
Al	4.58	2.9	5.1
Si	0.24	0.2	-
Cl	7.39	0.4	1.3
Zn	56.82	46.2	54.2
S	-	2.1	-
P	-	-	2.8

Zeta potential results

Electrical neutrality of the particles can be shown as following: Electrically neutral = Particle surface + first layer + second layer. When the particles in the bulk solution move, they cause particle shearing on the surface. Thereby, the neutrality of the particles on the diffuse layer changes and they gain a potential which is called zeta potential. In other words, it shows the potential difference between the shear plane (dispersed particle) of the sorbent and the bulk solution (dispersion medium) (Jafari et al., 2016).

The zeta potential plays a vital role to reveal the stability of the colloidal dispersions. High zeta potential (positive or negative) values indicate that the particles are electrically neutral, while the small ones refer the tendency to coagulate or flocculate (Greenwood and Kendall, 1999; Hanoar et al., 2012).

The Zeta potential was measured for the adsorbent to support the mechanism of the pH effect on the nutrient adsorption. An important criterion for the zeta potential graphs is the isoelectric

point (pH_{zpc}) where the potential changes from positive to negative values. For the synthesized Zn/Al-LDH, the isoelectric point was 10.06. The high isoelectric value suggests that the surface of the material is positive on a wide pH range and able to attract anions effectively.

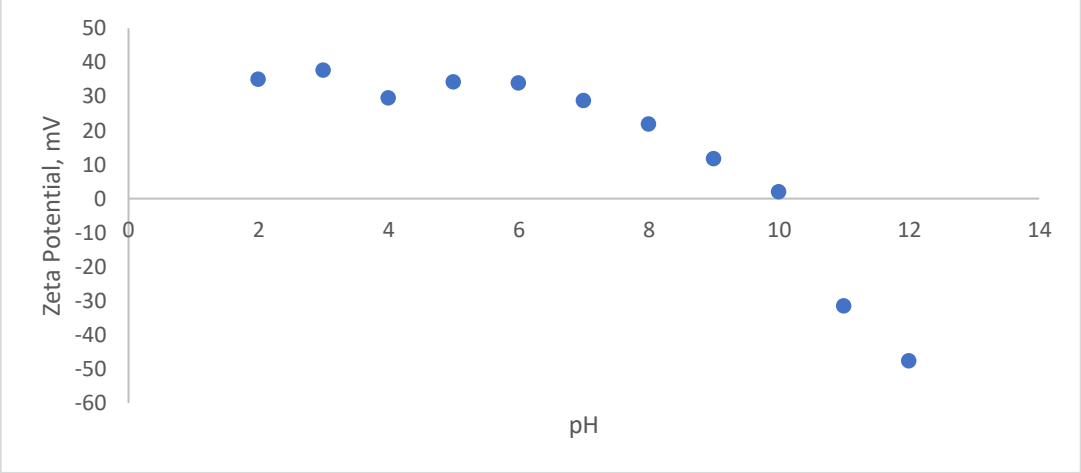

Figure 8. Zeta potential of Zn-Al/LDH adsorbent

BET surface area and adsorption – desorption Isotherms

Brunauer-Emmett-Teller (BET) theory is applied to reveal the adsorption of gas molecules on the sorbent surface and identify the specific surface area of the solid materials. Adsorbents with high surface area usually exhibit better adsorption performances. Therefore, the BET theory has a vital role of adsorbent design and selection. In BET methods, low temperature (77 K) gas adsorption process is followed and nitrogen gas is adsorbed due to its inert structure. From the adsorbed amount of nitrogen, it is possible to calculate the surface area of the adsorbent (Worch, 2012).

Nitrogen adsorption-desorption isotherm of the Zn-Al/LDH is illustrated in Figure 9. As it can be seen, the adsorbent exhibits type III isotherm which suggests the mesoporous structure with weak affinities. As being a mesoporous material, it has a pore diameter between 2 and 50 nm.

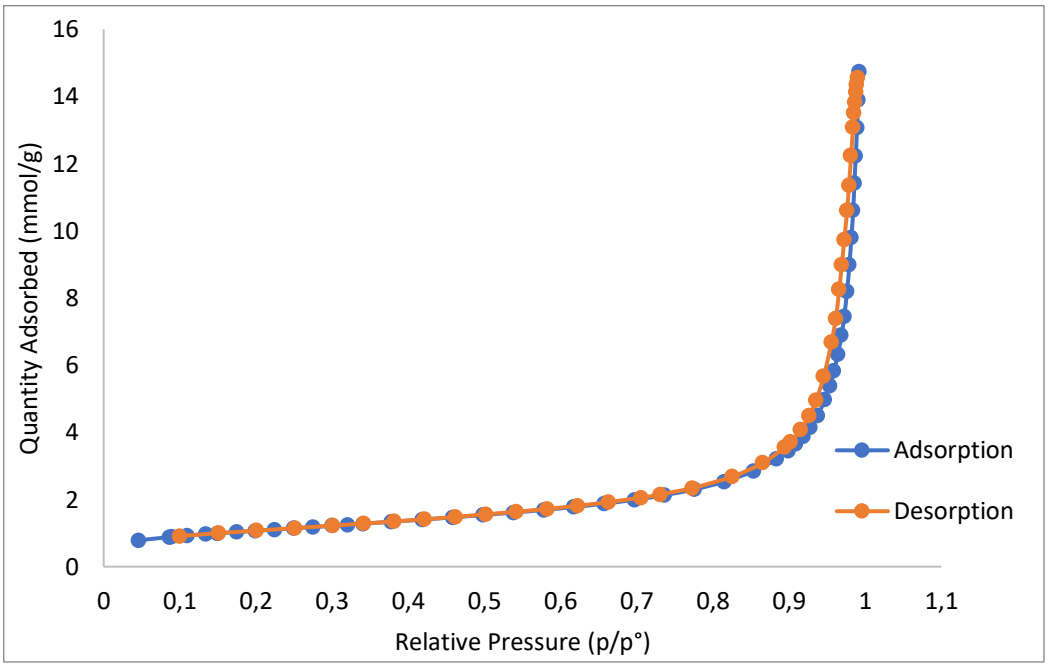

Figure 9. Nitrogen adsorption desorption graph of Zn-Al/LDH adsorbent

BET Surface area of the synthesized Zn/Al LDH was measured as 85.5 m^2/g and the results are provided below in Table 4 along with BET surface area of other reported LDH materials in the literature. It is clear from Table 3 that BET surface area of Zn/Al LDH is quite comparable with other reported LDH materials.

Table 4. Surface area values of synthesized LDH along with the other studies in literature

LDH type	BET surface area (m^2/g)	Pore volume (cm^3/g)	Average pore width (nm)	Reference
Zn/Al	**85.5**	**0.178**	**8.33**	**This study**
Ni/Mg/Al	101	0.590	23.4	Lei et al., 2017
Mg/Al	104	0.683	25.9	Yang et al., 2014
Zn/Al	135	0.151	4.42	Yang et al., 2014
Mg/Fe	65	0.530	307	Liu et al., 2014
Calcined Mg/Mn	84			Chitrakar et al., 2005

Mg/Al	109			Sepehr at al., 2014
ZnAl-LDHs/g-Al_2O_3	165	0.600		He et al., 2017
Mg/Al	84.5	0.33	15.8	Chubar et al., 2013
Zn/Al	50			Li et al., 2014
$Zr/Cr_2/NO_3$	20	0.05		Koilraj and Kannan, 2013
Calcined Mg/Al	198			Yang et al., 2005
Cl/Li/Al	18.8			Liu et al., 2006
Mg/Al	34.8			Lehmann et al., 1999

6. 2 Adsorption studies

As mentioned before, different LDH materials with different ratios and calcination temperatures were synthesized in this study and their sulfate removal performances are illustrated in Figure 10. According to Figure 10, Zn/Fe LDH does not exhibit a good removal performance in any ratio or calcination temperature. In terms of temperature, it is easily noticeable that uncalcined and 100ºC calcination temperature do not make any contribution. Zn/Al ratio as being another parameter shows that the ratio 3:1 and 4:1 have the highest rates. Finally, when overall results were taken into consideration, Zn/Al LDH calcined at 200 ºC with 4:1 Zn:Al ratio was selected for the more detailed experiments.

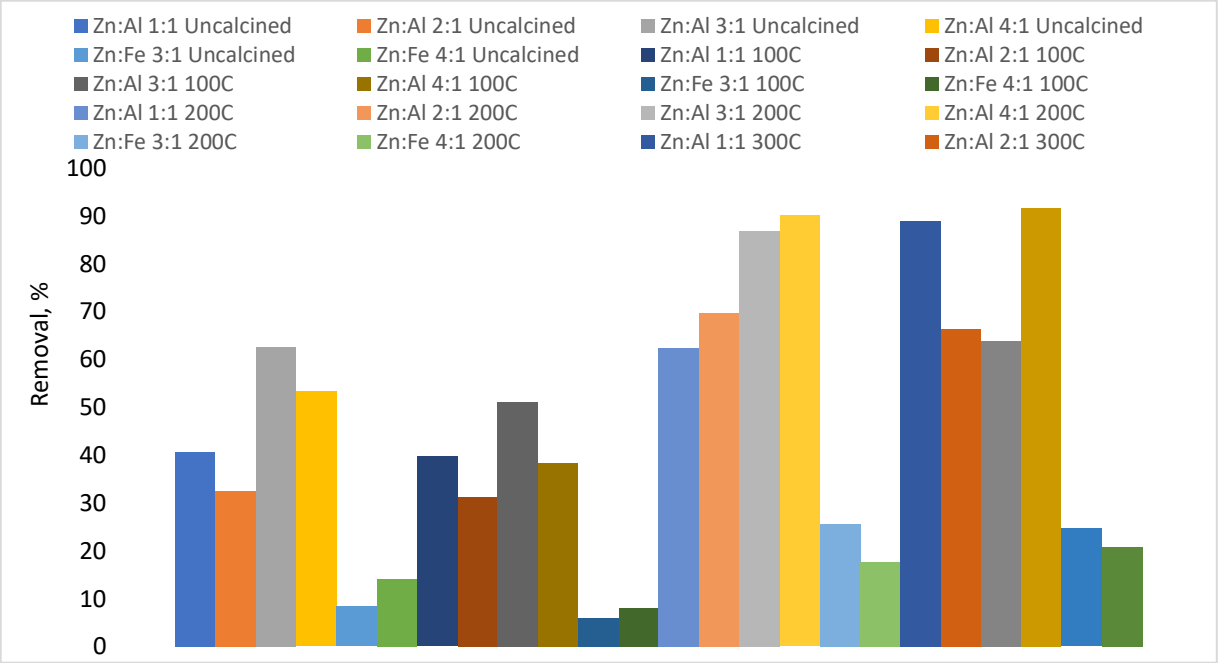

Figure 10. The sulfate removal performances of all synthesized adsorbents

Effect of solution pH

Sulfate and phosphate removal percentage studies were carried out at room temperature (25±2ºC) for 5 hours contact time. Initial concentrations were 118 mg sulfate/L and 116 mg phosphate/L with 1 g/L adsorbent dosage. The effect a wide pH range was studied in accordance with the purpose. The results are demonstrated in Figure 11.

As it can be seen from Figure 11, pH does not play an important role on adsorption capacity or removal rates of sulfate and phosphate. This result is also supported by the zeta potential analysis shown in Figure 9. However, there was a slight decrease with pH 8; therefore, the experiments were carried out with the initial pH values varying between 5 and 6. Additionally, it was found out that Zn/Al-LDH exhibited better removal rate and adsorption capacity for phosphate over sulfate. The decrease of both sulfate and phosphate adsorption with increasing pH is plausible since the competition for the available adsorption sites between the sulfate/phosphate and hydroxyl ions increase.

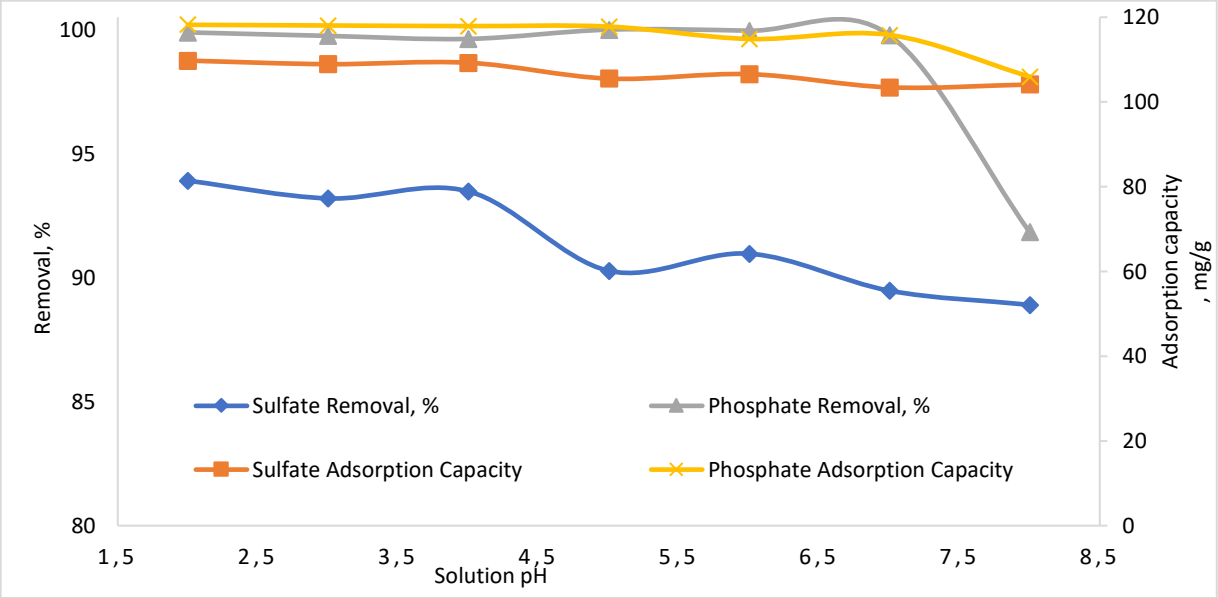

Figure 11. Effect of pH on sulfate removal rate and adsorption capacity

Effect of adsorbent dosage

Another important parameter is the dosage of the adsorbent as it is proportional to the cost of the processes. The optimum value was aimed to determine within these experiments where the adsorbents exhibit the best performance for both compounds. Figure 12, illustrates the effect of adsorbent dosage to the removal efficiency and adsorption capacity values for sulfate and phosphate. The initial concentrations were chosen as 148.4 mg sulfate/L and 115.3 mg phosphate/L. It shows the drastic effect of the adsorbent dosage, especially for sulfate recovery. Removal rate increased proportionally with the dosage for both compounds. However, as it was a comparative study for sulfate and phosphate 1.0 g/L dosage was chosen for the rest of the experiments as sulfate removal rate exceeded 90% at this value.

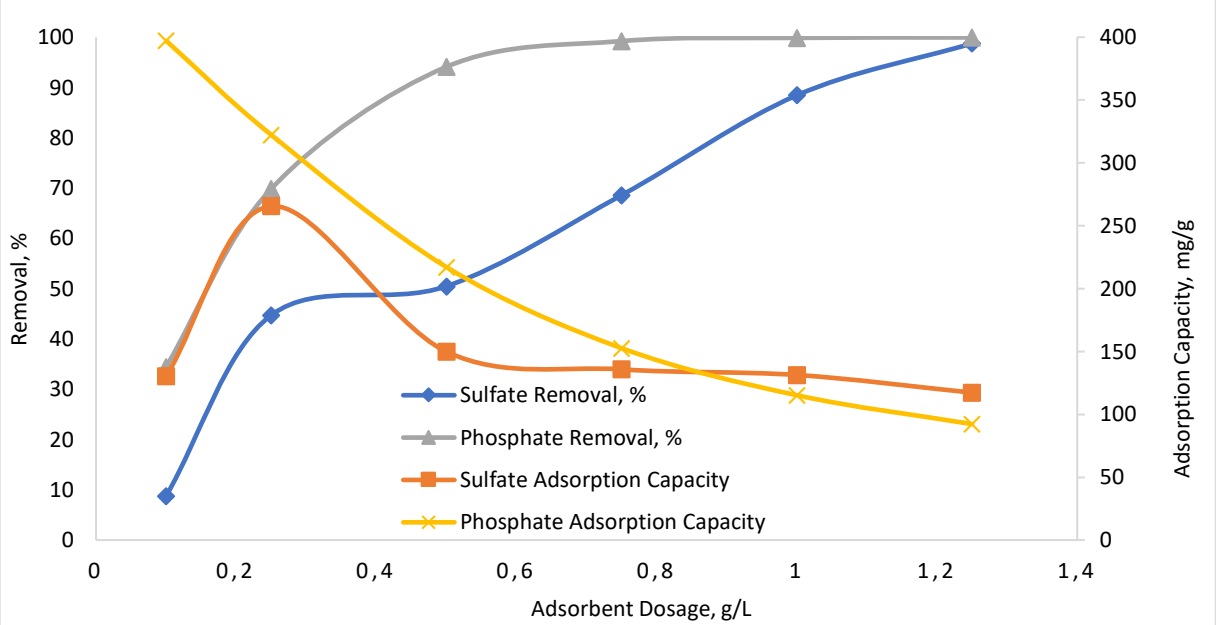

Figure 12. Effect of adsorbent dosage on sulfate removal rate and adsorption capacity

Effect of contact time and adsorption kinetics

All kinetic experiments were performed at 25ºC ±2 at 220 rpm shaker conditions. As mentioned before, five different concentrations with different contact times were investigated in order to obtain more accurate results with Pseudo-first, Pseudo-second, Interparticle Diffusion and Boyd's Diffusion Model. At first, the adsorption capacities and removal rates were demonstrated for different concentrated solutions.

i. Effect of contact time on sulfate removal

As seen in Figure 13 and Figure 14, removal rate decreased with the increase in the concentration of the solution. As it was decided to perform the other experiments with the sulfate concentration of approximately 117 mg/L, it is vital to emphasize the maximum removal rate of 91% in less than 5 hours with an adsorbent dosage of 1 g/L. In addition, the adsorption capacity of this concentration value was calculated as 106.5 mg sulfate/g adsorbent. However, the maximum adsorption capacity ascended to 119 mg/g with the higher concentrations.

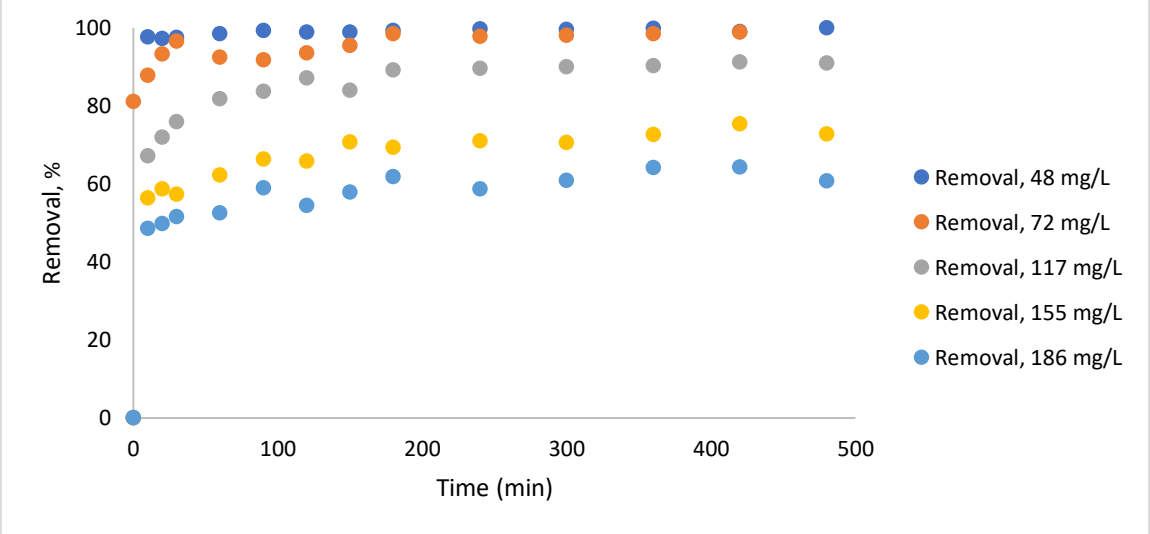

Figure 13. Removal rates for sulfate adsorption

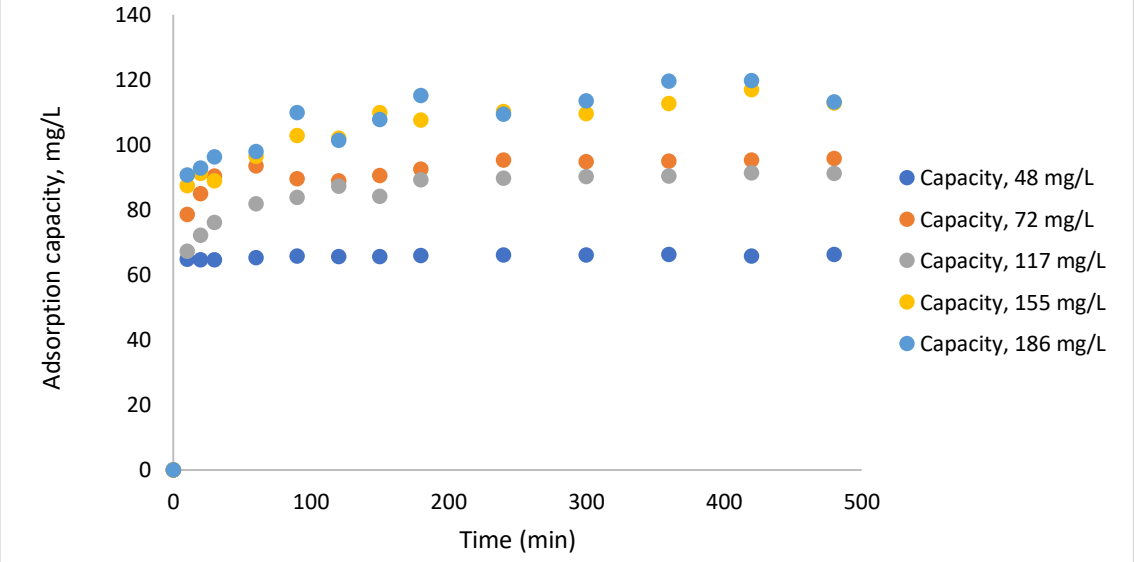

Figure 14. The effect of contact time on sulfate adsorption capacity

Finally, it is vital to mention that the results of this experiment group determined the required contact time during the rest of experiments. As it can be seen, after 5 hours there was no significant change in the removal rate; therefore, 5 hours was decided to be the optimum contact time for sulfate removal in order to minimize the time and energy consumed.

In Figure 15 and Figure 16, the four kinetic models of adsorption applied are illustrated with their equations. In Table 3, the calculated kinetic parameters for these models are represented.

There are two important criteria to determine the applicability of the model: the R^2 value and the discrepancy between the experimental maximum adsorption capacity and the one calculated by the aid of the model.

For adsorption modeling, both linearized and non-linear equations have widely been applied for experimental data fitting; however, according to many studies, non-linear equations provide more accurate results (Liubov, 2016, pp.45; Lin and Wang, 2009).

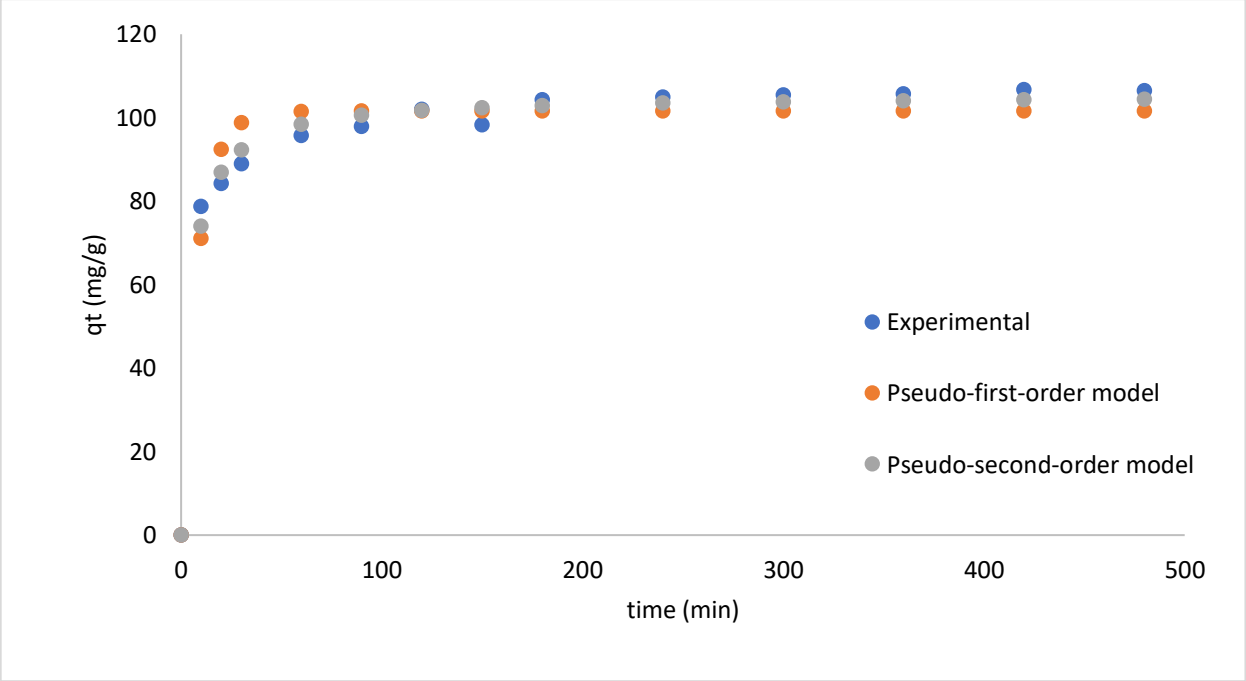

Figure 15. Pseudo-first and pseudo-second order model fittings for sulfate adsorption

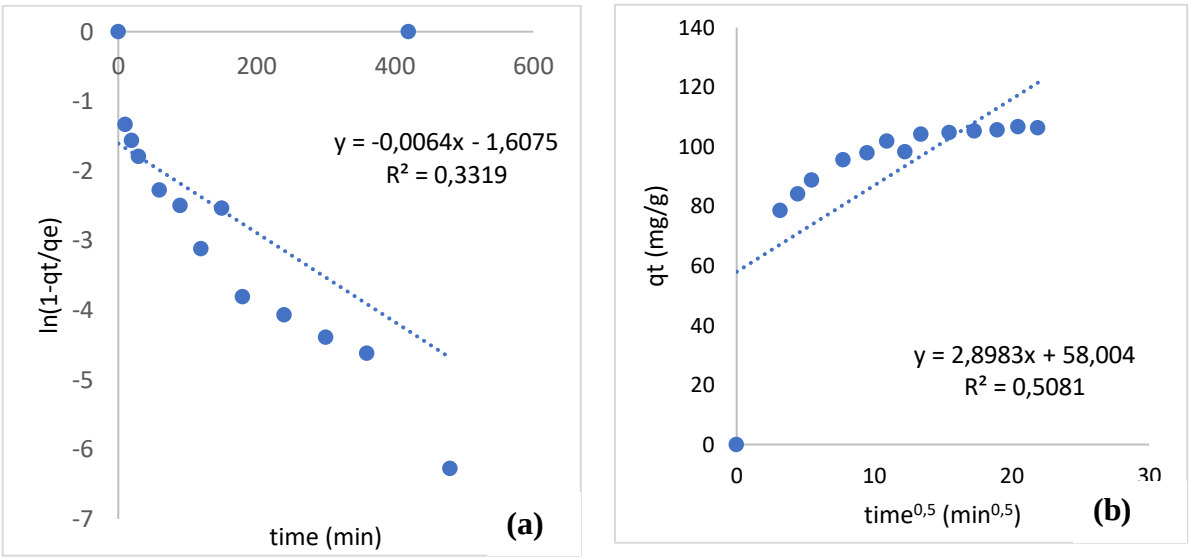

Figure 16. Boyd's diffusion model (a) and intra-particle model (b) fittings for sulfate removal

As shown in Figure 15, Figure 16 and Table 5, the pseudo-second-order kinetic model suits to the experimental system the most compared to the other ones based on its high R^2 value and small discrepancy between experimental (106.5 mg/g) and calculated maximum adsorption capacity values. These results show that the rate determining step is surface reaction.

The intra-particle diffusion plot suggests that the diffusion of sulfate occurs through multiple stages and plot of q_t versus $t^{1/2}$ did neither exhibit high reliability nor passed through the origin. Boyd model also did not pass through the origin even though its reliability was slightly better than the Intra-particle model.

Table 5. Calculated kinetic parameters for sulfate removal

Pseudo-first-order model		
R^2	k_1 (min^{-1})	q_e (mg/g)
0.981	0.1208	101.6
Pseudo-second-order model		
R^2	k_2 (min^{-1})	q_e (mg/g)
0.995	0.0023	105.3
Boyd's diffusion model		

R^2	B	
0.332	-0.006	
Intra-particle diffusion model		
R^2	C	k_i
0.508	58.0	2.89

ii. Phosphate removal

The effect of contact time on adsorption capacity for phosphate removal by means of Zn-Al/LDH is provided in Figure 17 and Figure 18. From the figures, it can be understood that the phosphate selectivity of Zn-Al/LDH is higher than sulfate as it has higher removal rates and adsorption capacity values. Since this work is a comparative study, approximately 118 mg/L phosphate solution was used during the rest of the experiments. > 99% removal rate and 161.7 mg/g maximum adsorption capacity were reached with 1g/L adsorbent dosage. Additionally, it can be predicted that higher adsorption capacity and adequate removal rates will be reached in the case of more concentrated phosphate solutions.

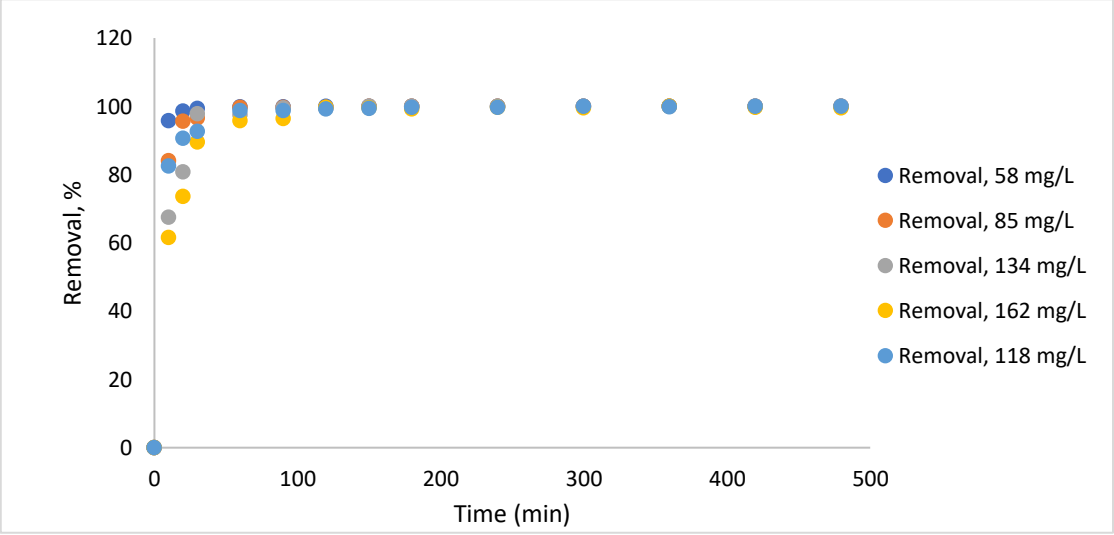

Figure 17. Phosphate removal rates as a function of time

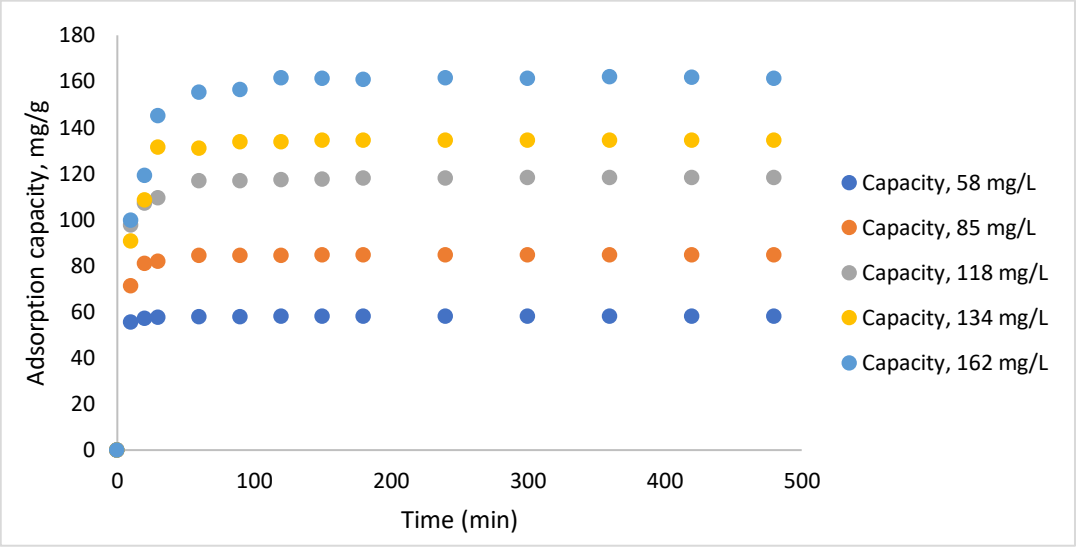

Figure 18. Effect of contact time to adsorption capacity for phosphate adsorption

Pseudo-first-order and pseudo-second-order model fittings for phosphate removal are illustrated below in Figure 19 along with the experimental results. Figure 20, shows Boyd and intra-particle diffusion model fittings.

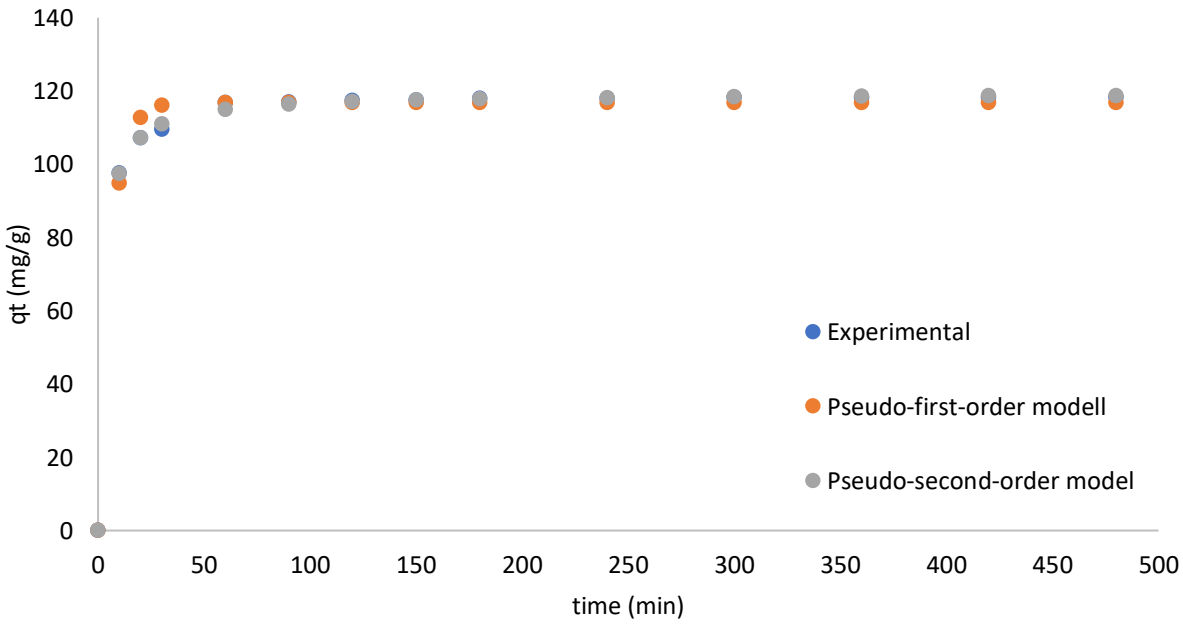

Figure 19. Pseudo-first and pseudo-second order model fittings for phosphate removal

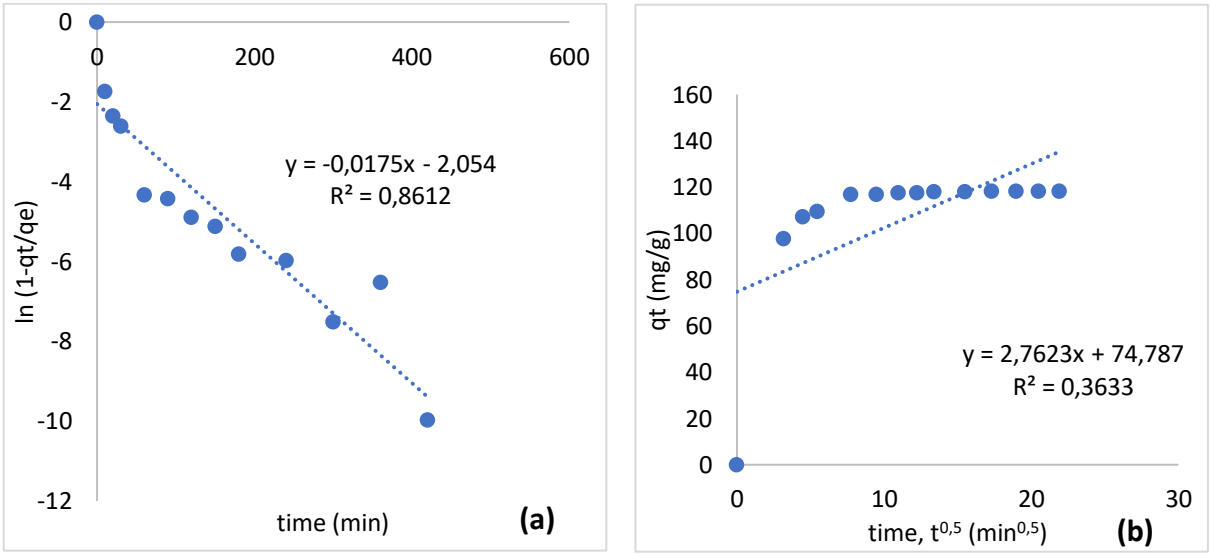

Figure 20. Boyd's diffusion model (a) and intra-particle model (b) fittings for phosphate removal

Boyd's model exhibited more reliable results with a R^2 value of 0.861; however, the linear line did not pass through the origin neither for Boyd nor intra-particle diffusion model. Among the studied reaction models, pseudo-second order model defines the mechanism better as it is more reliable with R^2 value of 0.995. Similar to sulfate removal, phosphate removal mechanism is also found to be controlled by the chemical reaction step.

Table 6. Kinetic model parameters for phosphate removal

Pseudo-first-order model		
R^2	k_1 (min^{-1})	q_e (mg/g)
0.981	0.167	116.8
Pseudo-second-order model		
R^2	k_2	q_e (mg/g)
0.995	0.0037	119.3
Boyd's diffusion model		
R^2	B	
0.861	-0.018	

Intra-particle diffusion model		
R^2	C	k_i
0.363	74.8	2.76

Based on the kinetic results the removal rate of phosphate was also slightly faster compared to that of sulfate. This is comparable to the earlier reported selectivity series for uptake of common inorganic anions by LDH materials (Halajnia et al., 2013).

Effect of initial concentration and adsorption isotherms

Adsorption isotherms are obtained at different aqueous equilibrium concentrations and at constant temperature and pressure to determine the adsorption potential of Zn-Al/LDH. In order to determine the isotherm model of synthesized LDH for sulfate and phosphate, 4 different temperatures (25 ºC, 35 ºC, 45 ºC and 55 ºC) were applied for a wide range on concentration varying between 29 mg/L and 290 mg/L. The Langmuir, Freundlich, Sips and Temkin isotherms were investigated within this study and the results are illustrated in the following figures.

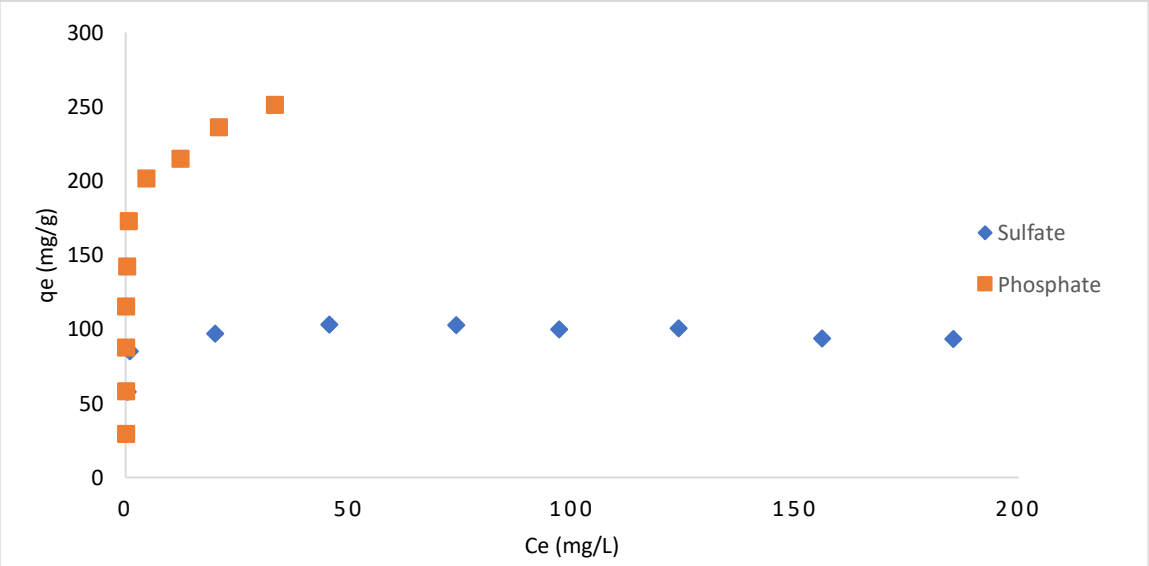

Figure 21. Adsorption isotherms of phosphate and sulfate onto Zn/Al-LDH

In Figure 21, the higher adsorption capacity for phosphate can be seen, as this value exceeds 250 mg/g while for sulfate 100 mg/g was reached as the highest value. In addition, lower removal rate for sulfate is once again corroborated by higher equilibrium concentrations.

Four isotherm models were investigated by the utilization of equilibrium data as following for sulfate and phosphate removal, respectively.

i. Sulfate removal

Figure 22 shows the adsorption isotherm results with experimental and model values. As can be seen, all three models except Temkin Model, showed good similarity against the experimental results.

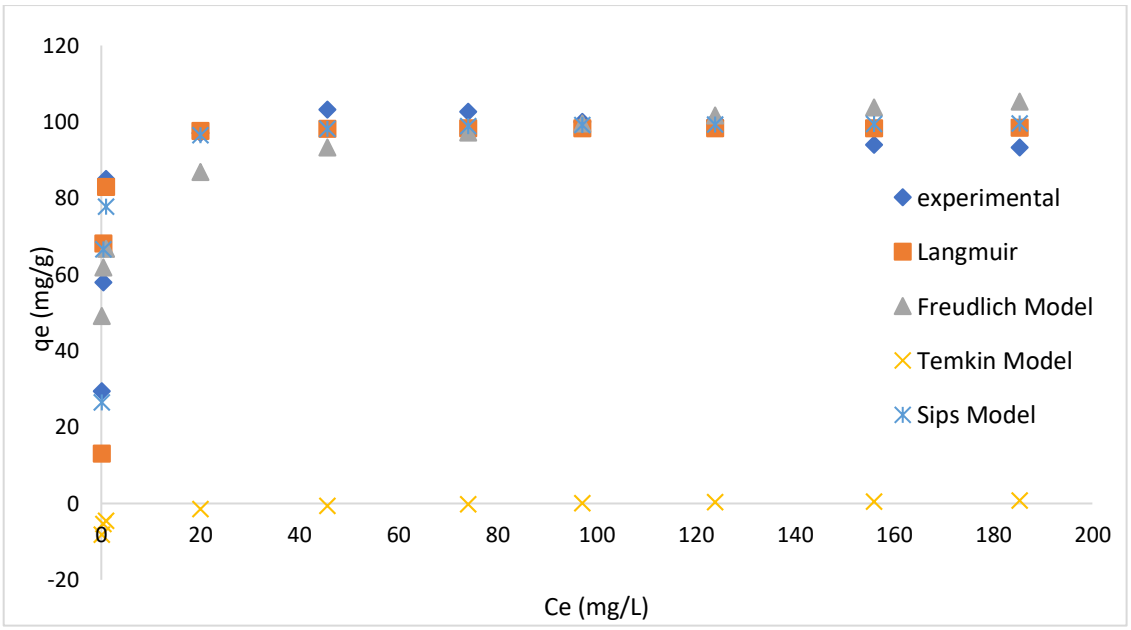

Figure 22. Adsorption isotherms of sulfate onto Zn-Al/LDH

However, as seen in Table 7, Sips isotherm surpasses the others in terms of maximum adsorption capacity vicinity and R^2 values. R^2 values descended in the order of Sips > Langmuir > Freundlich > Temkin. As being combination of Langmuir and Freundlich Isotherm models, Sips model often gives satisfactory results that fit the experimental data well, particularly when heterogeneous surface is involved. Finally, although Langmuir showed high reliability, Sips model gave slightly closer q_m values to the experimental capacity values. Therefore, Sips model was chosen to define the adsorption equilibrium in the terms of isotherm studies (Hokkanen et

al., 2014). The fitting of the Sips isotherm indicates that the adsorption system was heterogeneous.

Table 7. Isotherm model parameters for sulfate adsorption

Langmuir			
R^2	K_L(L/mg)	q_m (mg/g)	
0.969	5.64	98.44	
Freundlich			
R^2	K_f	n	
0.877	66.98	11.56	
Sips			
R^2	K_s	q_m (mg/g)	n
0.976	7.28	100.6	0.633
Temkin			
R^2	A (L/g)	B (J/mol)	
0.913	-	-	

ii. Phosphate removal

Adsorption isotherm of phosphate is shown in Figure 23. Sips and Langmuir Isotherm Models exhibited high performance to define the phosphate adsorption process onto Zn/Al-LDH. However, due its higher R^2 value and predicted adsorption capacity, Sips Model emerged as the best Model to define the system. R^2 values descended in the order of: Sips > Temkin > Langmuir >Freundlich. In addition to its higher R^2, Sips isotherm model approached to the experimental maximum capacity value better than the Langmuir model. The better fit of Sips isotherm to the experimental values can be explained with the fact that it takes three parameters into account.

In addition, the adsorbent exhibited better performance for phosphate removal compared to sulfate in Figure 21. Based on these results, higher phosphate concentrations could be studied with the synthesized adsorbent.

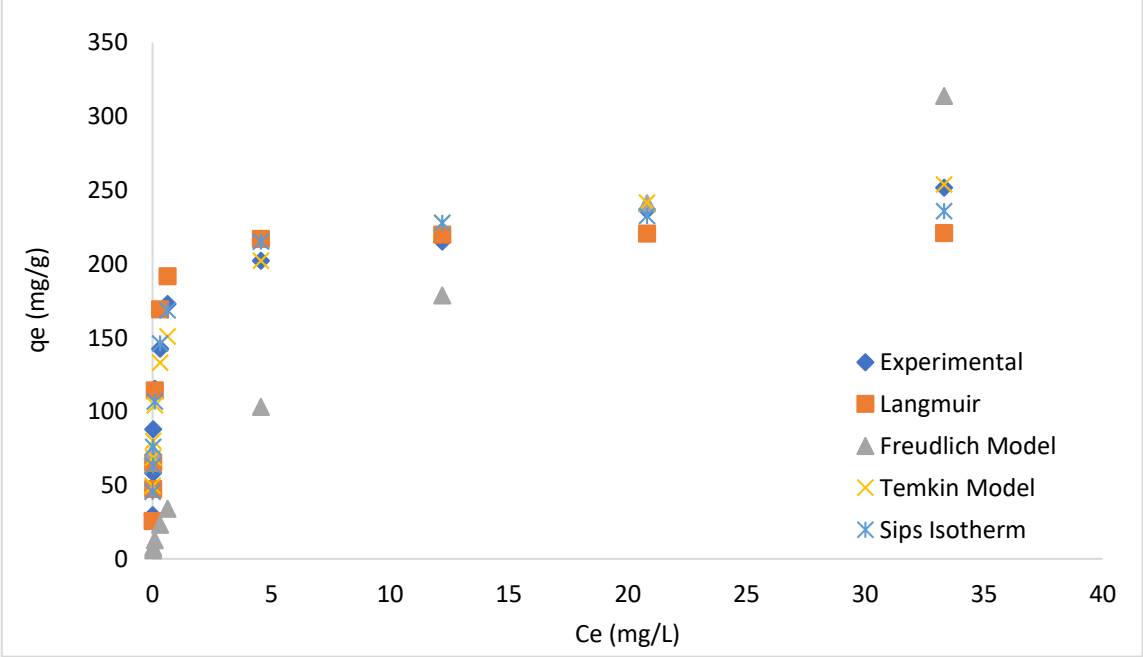

Figure 23. Langmuir plots for phosphate removal

Table 8. Isotherm model parameters for phosphate

Langmuir			
R^2	K_L (L/mg)	q_m (mg/g)	
0.972	10.04	221.5	
Freundlich			
R^2	K_f	n	
0.777	837.8	1.78	
Sips			
R^2	K_s (L/mg)	q_m (mg/g)	n
0.990	5.90	246.6	0.579
Temkin			

R^2	A (L/g)	B (J/mol)
0.986	521.3	25.9

Sorption mechanism

The adsorbent and the ion to be adsorbed play the most critical roles in the sorption mechanism. Commonly observed mechanisms for sulfate and phosphate are as follows: surface adsorption, interlayer anion exchange, reconstruction of the structure by the aid of memory effect, and precipitation. The determining factors for the mechanism are contact time, concentration and pH of the solution (Goh et al., 2008; Wan et al., 2016).

In the case of surface adsorption, an atomic film is formed due to the attachment of the components to be adsorbed to LDH surface. Layer charge density, which is defined as the electric charge on the surface for a certain area, plays an important role along with the anions in the interlayer (Goh et al., 2008).

Most common mechanisms for phosphate adsorption onto LDHs are shown in Figure 24 below.

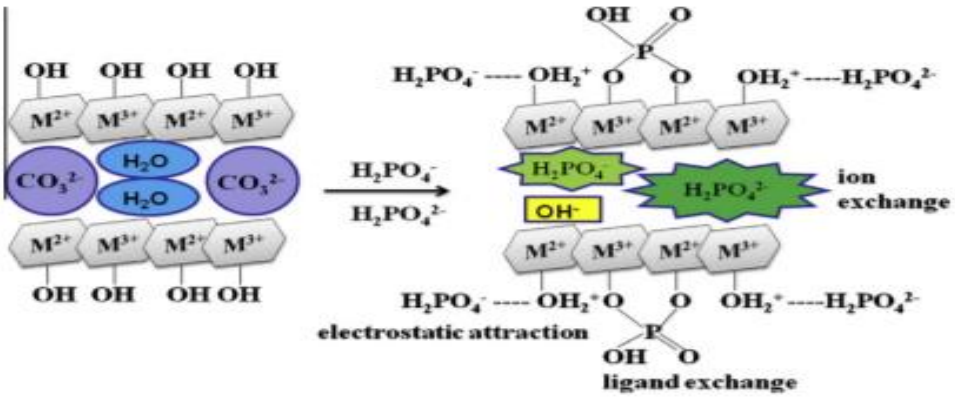

Figure 24. Possible mechanisms for phosphate adsorption onto LDH (Yang et al., 2014)

Sulfate and phosphate were exchanged with the hydroxyl groups that are represented with Cl- and then these ions were released to the solution in case of interlayer anion exchange mechanism. Therefore, it is the most plausible mechanism in the studied system due to the release of chloride ions into the solution during sulfate and phosphate uptake which is often the

case for LDH and is shown in the Figure 25 where there is a significant decrease in terms of chloride in the solid structure.

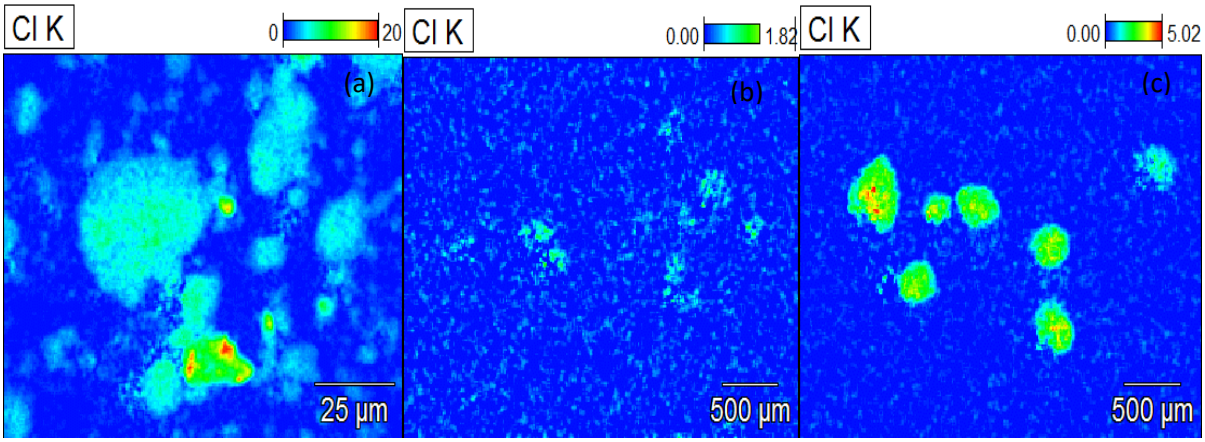

Figure 24. EDS chloride elemental mapping figures of raw ZnAl/LDH (a), after sulfate uptake (b) and after phosphate uptake (c)

Effect of temperature and adsorption thermodynamics

There are several thermodynamic parameters such as ΔG°, ΔH°, and ΔS° which are dependent on the temperature. Therefore, different temperature intervals were applied for revealing the adsorption thermodynamics of sulfate and phosphate adsorption by Zn/Al-LDH.

As mentioned before, Gibbs free energy can be calculated as following:

$$\Delta G° = -RTlnK_{ads} \qquad \text{(Equation 6.1)}$$

Where, $\Delta G°$ is the standard Gibbs free energy

R is universal gas constant

T is temperature

K_{ads} is equilibrium constant

R is a constant independent from any other parameters, while K_{ads} is dependent on the temperature; therefore, each condition with different temperature has its unique K_{ads} and the appropriate values must be used in the equation. In order to obtain K_{ads} following equation was applied for different temperatures.

$$K_{ads} = \frac{q_e}{C_e} \qquad \text{(Equation 6.2)}$$

Where, q_e is the equilibrium adsorption capacity for a given temperature, mg/g

C_e is the equilibrium concentration for a given temperature, mg/L

i. Sulfate removal

The effect of temperature is illustrated in Figure 26, where the change in the removal efficiency and adsorption capacity are provided for different concentrations. Ten different equilibrium concentrations denote the different sulfate concentrations in the experiments. As expected, the removal rate slightly increased with the temperature increase. However, there was no drastic change in the sulfate removal performance of the adsorbent; therefore, 25 ºC (298 K) can be stated as the optimum temperature for the sulfate removal.

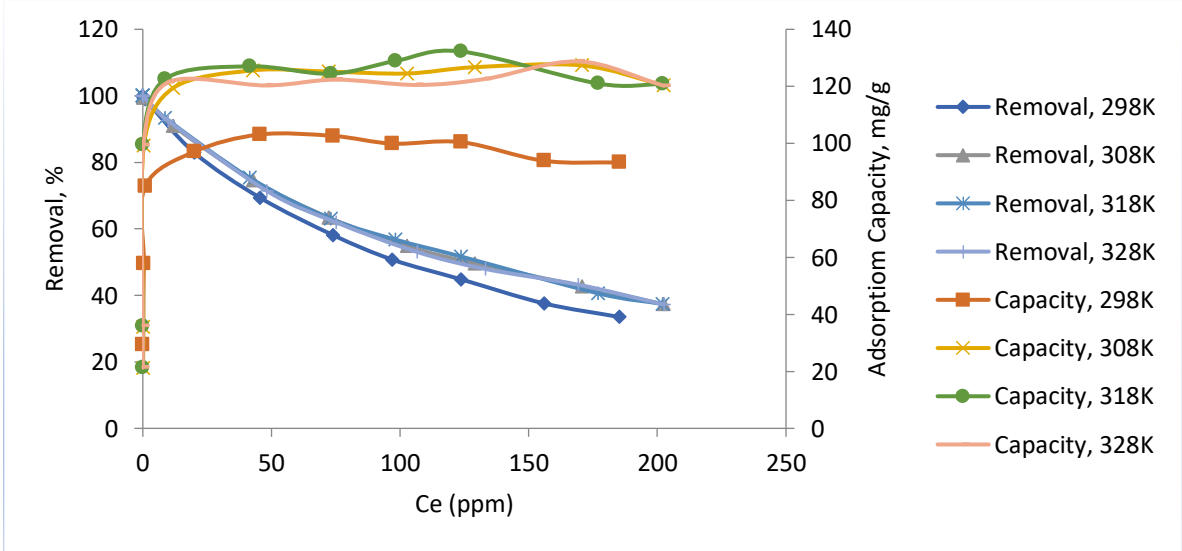

Figure 26. The effect of temperature to the sulfate removal rate and adsorption capacity

The thermodynamics of the adsorption process and thermodynamic variables were calculated as below.

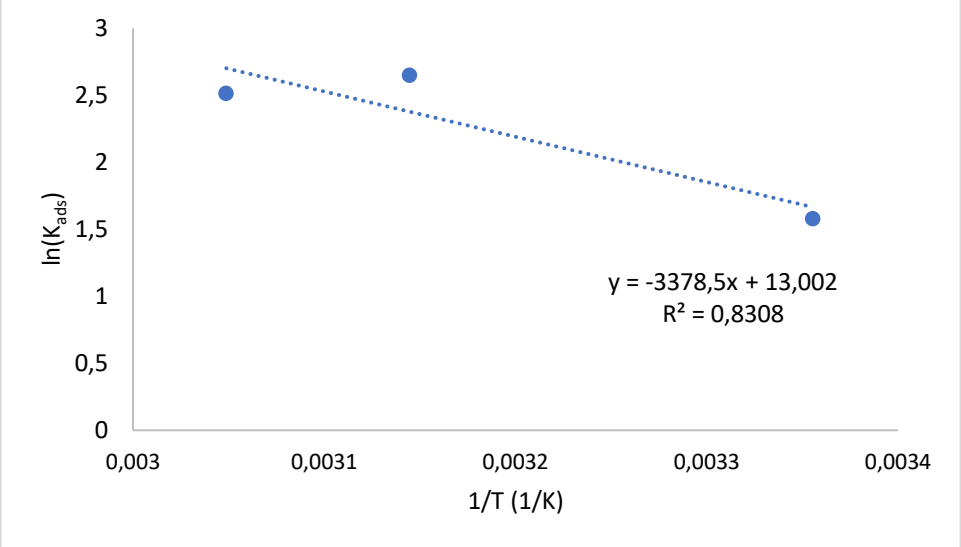

Figure 27. Van't Hoff plot for adsorption onto Zn-Al/LDH from sulfate solution

The equation of the graph is as following:

$$y=-3378.5x + 13.002$$

According to Van't Hoff equation:

$$\ln K_{ads} = -\frac{\Delta H^\circ}{R}T + \frac{\Delta S^\circ}{R} \qquad \text{(Equation 6.3)}$$

Entropy and enthalpy of the solutions were calculated from the intercept and slope of the equation, respectively. The obtained results are demonstrated in Table 9.

Table 9. Thermodynamic analysis of sulfate adsorption onto Zn/Al-LDH

T (K)	ΔH° (kJ/mol)	ΔS° (J/molK)	ΔG° (kJ/mol)
298	28.10	108.10	-3.914
318			-6.996
328			-6.859

i. Phosphate removal

The change in phosphate removal rates and adsorption capacity of the Zn-Al/LDH with the temperature are demonstrated in Figure 28 below.

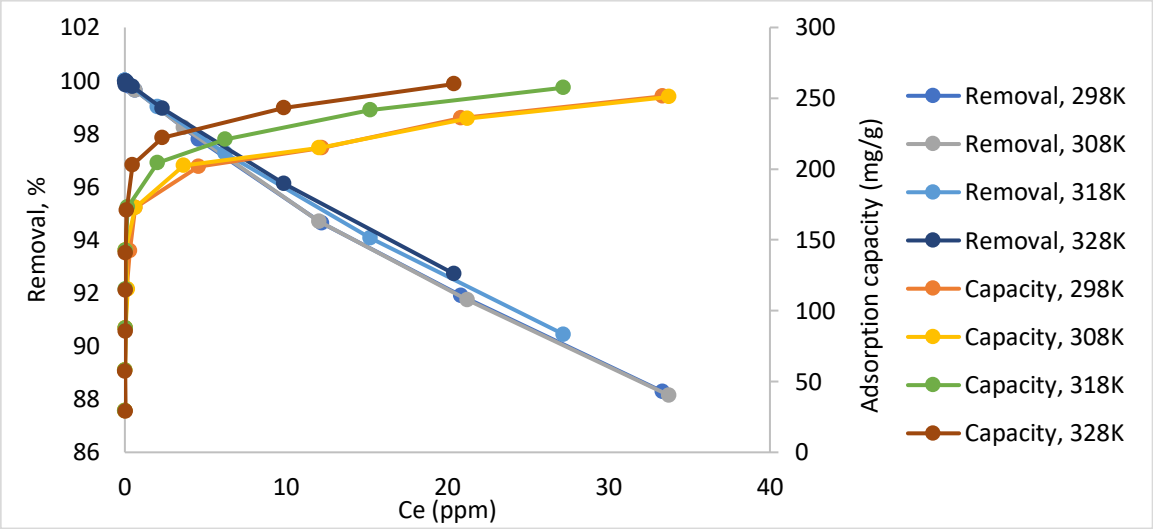

Figure 28. The effect of temperature to the phosphate removal rate and adsorption capacity

The variables were calculated similarly as sulfate adsorption as below:

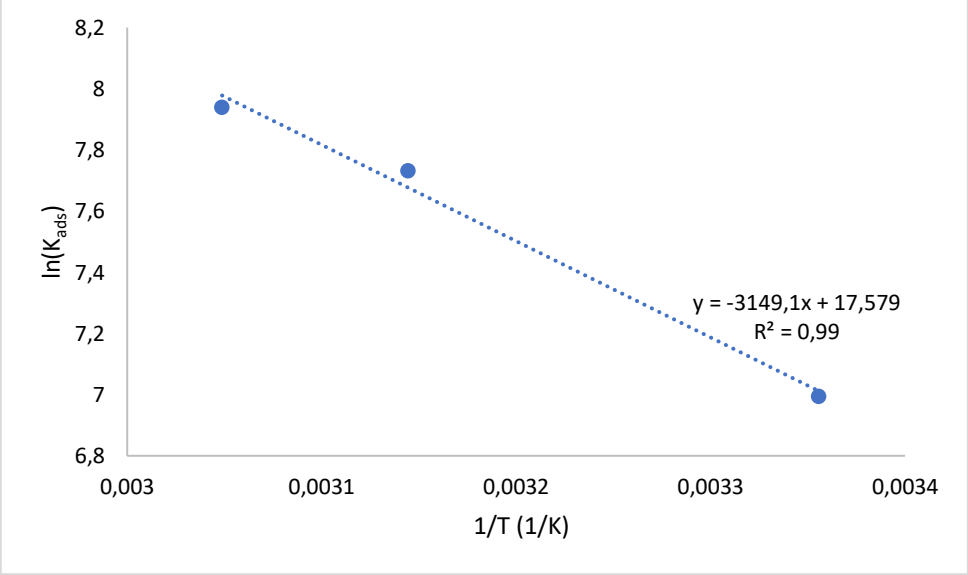

Figure 29. Van't Hoff plot for adsorption onto Zn-Al/LDH from phosphate solution

The equation of the graph is as following:

$$y=-3149.1x + 17.579$$

Similar to sulfate adsorption, with the application of equations 6.1, 6.2 and 6.3, following results were obtained for phosphate adsorption thermodynamic parameters:

Table 9. Thermodynamic analysis of phosphate adsorption onto Zn-Al/LDH

T (K)	ΔH° (kJ/mol)	ΔS° (J/molK)	$\Delta G°$ (kJ/mol)
298	26.18	146.15	-17.33
318			-18.49
328			-21.65

As known, positive values of ΔH° indicate the endothermic reaction, while exothermic reactions are taking place with negative values of ΔH°. Enthalpy values for both sulfate and phosphate are in parallel with the expected results as most of the adsorption processes are endothermic. Moreover, these positive enthalpies explain the proportional relationship between the temperature and the adsorbed amount of the pollutants. Entropy is the measurement of the randomness as its positive values indicate the increase in the randomness in the adsorption process. This increase has been connected to the release of hydrated water molecules during adsorption. Finally, the positive $\Delta G°$ values give the information that the adsorption is disfavored while negative values indicate the favored adsorption process and if it is equal to zero it means that the equilibrium conditions are reached. Based on this information, favored adsorption occurred for both sulfate and phosphate removal processes. Higher values of phosphate removal suggest higher attraction between LDH and phosphate compared to that between LDH and sulfate, which was also seen experimentally.

6. 3 Regeneration study

Reutilization is one of the most important criteria for the adsorbents, particularly for the removal / recovery of non-toxic components by reducing the costs significantly. The reusability of the adsorbent Zn/Al-LDH was revealed with the desorption and regeneration study. In accordance

with the purpose, nitric acid, hydrochloric acid, sodium hydroxide and NaCl were applied. The results of the regeneration study are shown in Table 10.

Table 10. Regeneration study results

Regenerate	Zn		Al		S			P		
	C_o, ppm	C_r, ppm	C_o, ppm	C_r, ppm	q_0, mg/g	q_r, mg/g	RE, %	q_0, mg/g	q_r, mg/g	RE, %
0.1M HCl	7.19	176	0	28	32.5	19.5	60.0	34.6	12.9	37.5
0.5 M HCl	6.97	177	0	29.3	32.8	19.44	59.3	34.7	13.3	38.4
0.1 M HNO_3	7.84	184	0	32.6	31.4	17.96	57.2	34.6	11.4	32.7
0.5 M HNO_3	7.93	178	0	29.7	32.1	21.04	65.6	34.7	15.3	44.2
0.1 M NaCl	7.79	6.4	0	0	32.5	27.1	83.1	34.6	34.5	99.6
0.5 M NaCl	7.37	3.6	0	0	31.3	16.03	51.1	34.6	34.3	99.2
0.1 M NaOH	7.29	35.7	0	45.5	32.9	10.83	32.8	34.6	0.59	1.71
0.5 M NaOH	7.42	174	0	35.5	30.9	16.96	54.8	34.5	3.13	9.06

Table 10 shows that the acidic and alkaline regeneration solutions did not work very well for the studied material most likely due to the collapse of the LDH structure in these rather harsh conditions. The best regeneration results for both sulfate and phosphate were obtained using 0.1 M NaCl. This means that during the regeneration chloride ions replaced the adsorbed anions converting the LDH structure again available for sulfate and phosphate adsorption. This fact also supports the anion exchange as the main removal mechanism in the studied system.

7. CONCLUSIONS

The main goal of this work was to inquire the sulfate and phosphate adsorption performances of layered double hydroxides as well as to establish the process parameters effects such as solution pH, contact time, temperature, and adsorbent dosage and to determine the best fitting kinetic and isotherm model.

Synthesized adsorbents were characterized by FTIR, XRD, SEM, EDS mapping, BET surface analyzer and zetasizer in order to verify the functional groups and surface morphology. The results confirmed the successful synthesis of the adsorbent.

Batch adsorption studies were performed in accordance with the above-mentioned purposes. The aim here was to reach the highest removal rates for sulfate and phosphate adsorption as well as to conduct a comparative study for these nutrients. Kinetic modeling revealed the rate determining step of the adsorption process. Adsorption isotherm models were applied to further understand the adsorption process and finally, the effect of temperature was established.

The main findings and the results of this thesis can be listed as follows:

1. Among the synthesized adsorbents 4:1 Zn:Al/LDH calcined at 200 °C exhibited the highest removal rate and the remaining experiments were carried out with this adsorbent.

2. The adequate removal rates for sulfate (>80%) and phosphate (>90%) were obtained with 1g/L adsorbent dosage for approximately 118 mg/L concentrations. In addition, the adsorption ability of the adsorbent was found to be very high for a large pH range from 2 to 8. Highest adsorption capacity values were found to be 119.6 mg sulfate/g and 161.7 mg phosphate/g.

3. The adsorption process reached the equilibrium conditions within 5 hours of contact time for both sulfate and phosphate ions. Kinetic study showed that adsorption of sulfate and phosphate ions followed the pseudo-second-order kinetic models which confirmed that the surface reactions were the rate determining step.

4. Adsorption isotherm models were applied and Sips Isotherm was found to be the most accurate model for both ions. Least square method error function was applied in the both kinetic and isotherm model fittings.

5. The predominant adsorption mechanism was suggested to be interlayer anion exchange. However, further studies such as FT-IR and XRD after the adsorption are needed for the verification of the mechanism.

6. The thermodynamic mechanism of the process was also revealed. Negative Gibbs Free Energy values indicated the favored process while positive enthalpy values were found as expected since the adsorption is an endothermic process.

7. For regeneration of adsorbent, 0.1 M NaCl solution was found to be the best desorbing medium.

The results of this thesis can be applied in the further studies for laboratory and pilot scale applications with both synthetic and real wastewater samples. On the other hand, challenges such as the negative effect of the calcination temperature must be taken into account and overcome. In addition, column studies can be carried out to confirm the stability of the solids and making granules might change the capacity and kinetic behavior of the adsorbents.

REFERENCES

Aharoni, C., Pasricha, N. and Sparks, D.L. (1992). Adsorption and desorption kinetics of cesium in an organic matter-rich soil saturated with different cations. *Soil Science*. 156, pp.233–239.

Ahmed, A., Talib, Z., Hussein, M. and Zakaria, A. (2012). Improvement of the crystallinity and photocatalytic property of zinc oxide as calcination product of Zn–Al layered double hydroxide. *Journal of Alloys and Compounds*, 539, pp.154-160.

Ai, L., Li, M. and Li, L. (2011). Adsorption of Methylene Blue from Aqueous Solution with Activated Carbon/Cobalt Ferrite/Alginate Composite Beads: Kinetics, Isotherms, and Thermodynamics. *Journal of Chemical & Engineering Data*, 56(8), pp.3475-3483.

Alkan, M., Demirbaş, Ö. and Doğan, M. (2007). Adsorption kinetics and thermodynamics of an anionic dye onto sepiolite. *Microporous and Mesoporous Materials*, 101(3), pp.388-396.

Apell, J.N. and Boyer, T.H. (2010). Combined ion exchange treatment for removal of dissolved organic matter and hardness. *Water Research*. 44, pp.2419-2430

Ashekuzzaman, S.M. and Jiang, J. (2017). Strategic phosphate removal/recovery by a re-usable Mg-Fe-Cl layered double hydroxide. *Process Safety and Environmental Protection*. 107, pp.454-462.

Asuquo, E., Martin, A., Nzerem, P., Siperstein, F. and Fan, X. (2017). Adsorption of Cd(II) and Pb(II) ions from aqueous solutions using mesoporous activated carbon adsorbent: Equilibrium, kinetics and characterization studies. *Journal of Environmental Chemical Engineering*, 5(1), pp.679-698.

Azizian, S. (2004). Kinetic models of sorption: a theoretical analysis. *Journal of Colloid and Interface Science*, 276(1), pp.47-52.

Bakr, A., Mostafa, M. and Sultan, E. (2016). Mn(II) removal from aqueous solutions by Co/Mo layered double hydroxide: Kinetics and thermodynamics. *Egyptian Journal of Petroleum*, 25(2), pp.171-181.

Barahuie, F., Hussesin, M.Z., Arulselvan, P., Fakurazi, S. and Zainal, Z. (2014). Drug delivery system for an anticancer agent, chlorogenate-Zn/Al-layered double hydroxide nanohybrid synthesized using direct co-precipitation and ion exchange methods. *Journal of Solid State Chemistry*, 217, pp.31-41

Basu, D., Das, A., Stöckelhuber, K., Wagenknecht, U. and Heinrich, G. (2014). Advances in layered double hydroxide (LDH)-based elastomer composites. *Progress in Polymer Science*, 39(3), pp.594-626.

Benatti, C.B., Tavares, C.R.G. and Lenzi, E. (2009). Sulfate removal from waste chemicals by precipitation. *Journal of Environmental Management*. 90(1), pp. 504-511

Bish, D.L. (1980). Anion exchange in takovite: applications to other hydroxide minerals. *Bone Minerals.* 103, pp.170-175

Bódalo, A., Gómez , J., Gómez, E., León, G and Tejera, M. (2004). Reduction of sulfate content in aqueous solutions by reverse osmosis using cellulose acetate membranes. Desalination. 162, pp.55-60

Cai, X., Shen, X., Ma, L., Ji, Z., Xu, C. and Yuan, A. (2015). Solvothermal synthesis of NiCo-layered double hydroxide nanosheets decorated on RGO sheets for high performance supercapacitor. *Chemical Engineering Journal*, 268, pp.251-259.

Cao, D., Zeng, H., Yang, B. and Zhao, X. (2017). Mn assisted electrochemical generation of two-dimensional Fe-Mn layered double hydroxides for efficient Sb(V) removal. *Journal of Hazardous Materials*, 336, pp.33-40.

Cardoso, L. and Valim, J. (2006). Study of acids herbicides removal by calcined Mg-Al-CO_3LDH. *Journal of Physics and Chemistry of Solids*, 67(5-6), pp.987-993.

Cavani, F., Trifirò, F. and Vaccari, A. (1991). Hydrotalcite-type anionic clays: Preparation, properties and applications. *Catalysis Today*, 11(2), pp.173-301.

Chen, H., Qian, G., Ruan, X. and Frost, R. (2016). Removal process of nickel(II) by using dodecyl sulfate intercalated calcium aluminum layered double hydroxide. *Applied Clay Science*, 132-133, pp.419-424.

Chen, L., Li, C., Wei, Y., Zhou, G., Pan, A., Wei, W. and Huang, B. (2016). Hollow LDH nanowires as excellent adsorbents for organic dye. *Journal of Alloys and Compounds*, 687, pp.499-505.

Chen, S., Xu, Z., Zhang, Q., Lu, G., Hao, Z. and Liu, S. (2009). Studies on adsorption of phenol and 4-nitrophenol on MgAl-mixed oxide derived from MgAl-layered double hydroxide. *Separation and Purification Technology*, 67(2), pp.194-200.

Chen, X., Fu, C., Wang, Y., Yang, W. and Evans, D. (2008). Direct electrochemistry and electrocatalysis based on a film of horseradish peroxidase intercalated into Ni–Al layered double hydroxide nanosheets. *Biosensors and Bioelectronics*, 24(3), pp.356-361.

Chitrakar, R., Tezuka, S., Sonoda, A., Sakane, K., Ooi, K. and Hirotsu, T. (2005). Adsorption of phosphate from seawater on calcined MgMn-layered double hydroxides. *Journal of Colloid and Interface Science*, 290(1), pp.45-51.

Chuang, Y., Tzou, Y., Wang, M., Liu, C. and Chiang, P. (2008). Removal of 2-Chlorophenol from Aqueous Solution by Mg/Al Layered Double Hydroxide (LDH) and Modified LDH. *Industrial & Engineering Chemistry Research*, 47(11), pp.3813-3819.

Chubar, N., Gerda, V., Megantari, O., Mičušík, M., Omastova, M., Heister, K., Man, P. and Fraissard, J. (2013). Applications versus properties of Mg–Al layered double hydroxides provided by their syntheses methods: Alkoxide and alkoxide-free sol–gel syntheses and hydrothermal precipitation. *Chemical Engineering Journal*, 234, pp.284-299.

Chubar, N., Gilmour, R., Gerda, V., Mičušík, M., Omastova, M., Heister, K., Man, P., Fraissard, J. and Zaitsev, V. (2017). Layered double hydroxides as the next generation inorganic anion exchangers: Synthetic methods versus applicability. *Advances in Colloid and Interface Science*.

Czelej, K., Cwieka, K. and Kurzydlowski, K. (2016). CO_2 stability on the Ni low-index surfaces: van der Waals corrected DFT analysis. *Catalysis Communications*, 80, pp.33-38.

Das, J., Patra, B., Baliarsingh, N. and Parida, K. (2006). Adsorption of phosphate by layered double hydroxides in aqueous solutions. *Applied Clay Science*, 32(3-4), pp.252-260.

Das, N., Konar, J., Mohanta, M. and Srivastava, S. (2004). Adsorption of Cr (VI) and Se (IV) from their aqueous solutions onto Zr^{4+}-substituted ZnAl/MgAl-layered double hydroxides: effect of Zr^{4+} substitution in the layer. *Journal of Colloid and Interface Science*, 270(1), pp.1-8.

Daud, M., Kamal, M., Shehzad, F. and Al-Harthi, M. (2016). Graphene/layered double hydroxides nanocomposites: A review of recent progress in synthesis and applications. *Carbon*, 104, pp.241-252.

Dou, W., Zhou, Z., Jiang, L., Jiang, A., Huang, R., Tian, X., Zhang, W. and Chen, D. (2017). Sulfate removal from wastewater using ettringite precipitation: Magnesium ion inhibition and process optimization. *Journal of Environmental Management*, 196, pp.518-526.

Do, D. (2008). *Adsorption analysis*. 1st ed. London: Imperial College Press.

Du, D., Ye, X., Zhang, J., Zeng, Y., Tu, H., Zhang, A. and Liu, D. (2008). Stripping voltammetric analysis of organophosphate pesticides based on solid-phase extraction at zirconia nanoparticles modified electrode. *Electrochemistry Communications*, 10(5), pp.686-690.

Duan, X. and Evans, D. (2006). *Layered double hydroxides*. Berlin: Springer.

Foo, K. and Hameed, B. (2010). Insights into the modeling of adsorption isotherm systems. *Chemical Engineering Journal*, 156(1), pp.2-10.

Fu, L., Wang, J. and Su, Y. (2009). Removal of low concentrations of hardness ions from aqueous solutions using electrodeionization process. *Separation and Purification Technology*. 68, pp. 390-396.

Gao, Z., Xie, S., Zhang, B., Qiu, X. and Chen, F. (2017). Ultrathin Mg-Al layered double hydroxide prepared by ionothermal synthesis in a deep eutectic solvent for highly effective boron removal. *Chemical Engineering Journal*, 319, pp.108-118.

Goh, K., Lim, T. and Dong, Z. (2008). Application of layered double hydroxides for removal of oxyanions: A review. *Water Research*, 42(6-7), pp.1343-1368.

Goh, K., Lim, T. and Dong, Z. (2009). Enhanced Arsenic Removal by Hydrothermally Treated Nanocrystalline Mg/Al Layered Double Hydroxide with Nitrate Intercalation. *Environmental Science & Technology*, 43(7), pp.2537-2543.

Gordon, J., Kazemian, H. and Rohani, S. (2012). Rapid and efficient crystallization of MIL-53(Fe) by ultrasound and microwave irradiation. *Microporous and Mesoporous Materials*, 162, pp.36-43.

Greenwood, R. and Kendall, K (1999). Electroacoustic studies of moderately concentrated colloidal suspensions. *Journal of the European Ceramic Society*. 19(4), pp.479–488.

Gürses, A., Hassani, A., Kıranşan, M., Açışlı, Ö. and Karaca, S. (2014). Removal of methylene blue from aqueous solution using by untreated lignite as potential low-cost adsorbent: Kinetic, thermodynamic and equilibrium approach. *Journal of Water Process Engineering*, 2, pp.10-21.

Halajnia, A., Oustan, S., Najafi, N., Khataee, A. and Lakzian, A. (2013). Adsorption–desorption characteristics of nitrate, phosphate and sulfate on Mg–Al layered double hydroxide. *Applied Clay Science*, 80-81, pp.305-312.

Hameed, B., Tan, I. and Ahmad, A. (2008). Adsorption isotherm, kinetic modeling and mechanism of 2,4,6-trichlorophenol on coconut husk-based activated carbon. *Chemical Engineering Journal*, 144(2), pp.235-244.

Hanaor, D.A.H., Michelazzi, M., Leonelli, C. and Sorrell, C.C. (2012). The effects of carboxylic acids on the aqueous dispersion and electrophoretic deposition of ZrO_2.*Journal of the European Ceramic Society*. 32(1), pp.235–244.

Hassan, H., Mohamad, A., Alyousef, Y. and Al-Ansary, H. (2015). A review on the equations of state for the working pairs used in adsorption cooling systems. *Renewable and Sustainable Energy Reviews*, 45, pp.600-609.

Hassan, H. and Mohamad, A. (2012). A review on solar-powered closed physisorption cooling systems. *Renewable and Sustainable Energy Reviews*, 16(5), pp.2516-2538.

He, H., Kang, H., Ma, S., Bai, Y. and Yang, X. (2010). High adsorption selectivity of ZnAl layered double hydroxides and the calcined materials toward phosphate. *Journal of Colloid and Interface Science*, 343(1), pp.225-231.

He, J., Yang, Z., Zhang, L., Li, Y. and Pan, L. (2017). Cu supported on ZnAl-LDHs precursor prepared by in-situ synthesis method on γ-Al_2O_3 as catalytic material with high catalytic activity for methanol steam reforming. *International Journal of Hydrogen Energy*, 42(15), pp.9930-9937.

Hesselmann, R., Hummell, R., Resnick, S., Hany, R. and Zehnder, A. (2000). Anaerobic metabolism of bacteria performing enhanced biological phosphate removal. *Water Research*, 34(14), pp.3487-3494.

Ho, Y. (2000). The kinetics of sorption of divalent metal ions onto sphagnum moss peat. *Water Research*, 34(3), pp.735-742.

Hokkanen, S., Repo, E., Bhatnagar, A., Tang, W. and Sillanpää, M. (2014). Adsorption of hydrogen sulphide from aqueous solutions using modified nano/micro fibrillated cellulose. *Environmental Technology*, 35(18), pp.2334-2346.

Hong, J., Zhu, Z., Lu, H. and Qiu, Y. (2014). Synthesis and arsenic adsorption performances of ferric-based layered double hydroxide with α-alanine intercalation. *Chemical Engineering Journal*, 252, pp.267-274.

Huang, W., et al., Adsorptive removal of phosphate from water using mesoporous materials: A review, Journal of Environmental Management (2017)

Iftekhar, S., Srivastava, V. and Sillanpää, M. (2017). Synthesis and application of LDH intercalated cellulose nanocomposite for separation of rare earth elements (REEs). *Chemical Engineering Journal*, 309, pp.130-139.

Inyang, H.I., Onwawoma, A. and Bae, S. (2016). The Elovich equation as a predictor of lead and cadmium sorption rates on contaminant barrier minerals. Soil & Tillage Research. 155, pp.124-132

Jafari, S. (2016). *Investigation of Adsorption of Dyes Onto Modified Titanium Dioxide*. Ph.D. Lappeenranta University of Technology.

Jafari, S., Tryba, B., Kusiak-Nejman, E., Kapica-Kozar, J., Morawski, A. and Sillanpää, M. (2016). The role of adsorption in the photocatalytic decomposition of Orange II on carbon-modified TiO2. *Journal of Molecular Liquids*, 220, pp.504-512.

Jaiswal, A., Mani, R., Banerjee, S., Gautam, R. and Chattopadhyaya, M. (2015). Synthesis of novel nano-layered double hydroxide by urea hydrolysis method and their application in removal of chromium(VI) from aqueous solution: Kinetic, thermodynamic and equilibrium studies. *Journal of Molecular Liquids*, 202, pp.52-61.

Jiang, F., Beck, M.B., Cummings, R.G., Rowles, K. and Russell, D. (2004). Estimation of costs of phosphorus removal in wastewater treatment facilities: Construction de Novo.

Júnior, O.K., Gurgel, L.V.A. and Gil, L.F. (2010). Removal of Ca (II) and Mg(II) from aqueous single metal solutions by mercerized cellulose and mercerized sugarcane bagasse grafted with EDTA dianhydride (EDTAD). Carbohydrate Polymers. 79(1), pp. 184-191

Kameda, T., Oba, J. and Yoshioka, T. (2015). Recyclable Mg–Al layered double hydroxides for fluoride removal: Kinetic and equilibrium studies. *Journal of Hazardous Materials*, 300, pp.475-482.

Kijjanapanich, P., Annachhatre, A.P., Esposito, G., van Hullebusch, E.D. and Lens, P.N.L., (2013). Biological sulfate removal from gypsum contaminated construction and demolition debris. *Journal of Environental Management*. 131, pp.82-91.

Kinniburgh, D. (1986). General purpose adsorption isotherms. *Environmental Science & Technology*, 20(9), pp.895-904.

Koilraj, P. and Kannan, S. (2013). Aqueous fluoride removal using ZnCr layered double hydroxides and their polymeric composites: Batch and column studies. *Chemical Engineering Journal*, 234, pp.406-415.

Koilraj, P. and Sasaki, K. (2016). Fe_3O_4/MgAl-NO_3layered double hydroxide as a magnetically separable sorbent for the remediation of aqueous phosphate. *Journal of Environmental Chemical Engineering*, 4(1), pp.984-991.

Ladewig, K., Xu, Z. and Lu, G. (2009). Layered double hydroxide nanoparticles in gene and drug delivery. *Expert Opinion on Drug Delivery*, 6(9), pp.907-922.

Largitte, L. and Pasquier, R. (2016). A review of the kinetics adsorption models and their application to the adsorption of lead by an activated carbon. *Chemical Engineering Research and Design*, 109, pp.495-504.

Lee, K., Nam, J., Lee, J., Lee, Y., Cho, S., Jung, C., Choi, H., Chang, Y., Kwon, Y. and Nam, J. (2005). Methanol and proton transport control by using layered double hydroxide nanoplatelets for direct methanol fuel cell. *Electrochemistry Communications*, 7(1), pp.113-118.

Lefebvre, D. and Tezel, F. (2017). A review of energy storage technologies with a focus on adsorption thermal energy storage processes for heating applications. *Renewable and Sustainable Energy Reviews*, 67, pp.116-125.

Legrouri, A., Lakraimi, M., Barroug, A., De Roy, A. and Besse, J. (2005). Removal of the herbicide 2,4-dichlorophenoxyacetate from water to zinc–aluminium–chloride layered double hydroxides. *Water Research*, 39(15), pp.3441-3448.

Lehmann, M., Zouboulis, A. and Matis, K. (1999). Removal of metal Ions from dilute aqueous solutions: A comparative study of inorganic sorbent materials. *Chemosphere*, 39(6), pp.881-892.

Lei, C., Zhu, X., Zhu, B., Jiang, C., Le, Y. and Yu, J. (2017). Superb adsorption capacity ofhierarchical calcined Ni/Mg/Al layered double hydroxides for Congo red and Cr (VI) ions. Journal of Hazardous Materials, 321, pp.801-811

Li, C., Wei, M., Evans, D. and Duan, X. (2014). Layered Double Hydroxide-based Nanomaterials as Highly Efficient Catalysts and Adsorbents. *Small*, 10(22), pp.4469-4486.

Li, D., Wang, H., Wang, L. and Zhao, Z. (2008). Removal of sulfate from aqueous solution by adsorption of it on layered double hydroxides.*Acta MineralogicaSinica.* 2, pp.109-114

Li, R., Wang, J., Zhou, B., Awasthi, M., Ali, A., Zhang, Z., Gaston, L., Lahori, A. and Mahar, A. (2016). Enhancing phosphate adsorption by Mg/Al layered double hydroxide functionalized biochar with different Mg/Al ratios. *Science of The Total Environment*, 559, pp.121-129.

Li, S., Bai, Z. and Zhao, D. (2013). Characterization and friction performance of Zn/Mg/Al-CO_3 layered double hydroxides. *Applied Surface Science*, 284, pp.7-12.

Li, Z., Yang, B., Zhang, S., Wang, B. and Xue, B. (2014). A novel approach to hierarchical sphere-like ZnAl-layered double hydroxides and their enhanced adsorption capability. *Journal of Materials Chemistry A*, 2(26), pp.10202-10210

Liang, X., Zang, Y., Xu, Y., Tan, X., Hou, W., Wang, L. and Sun, Y. (2013). Sorption of metal cations on layered double hydroxides. *Colloids and Surfaces A: Psychochemical Engineering Aspects*, 433, pp.122-131

Liubov, L. (2016). *Rare-earth metals adsorption on a novel bisphosphonate separation material*. Master's Thesis. Lappeenranta University of Technology.

Liu, J., Yue, X., Yu, Y. and Guo, Y. (2014). Adsorption of sulfate from natural water on calcined Mg–Fe layered double hydroxides. *Desalination and Water Treatment*, 56(1), pp.274-283.

Liu, Y. and Liu, Y. (2008). Biosorption isotherms, kinetics and thermodynamics. *Separation and Purification Technology*, 61(3), pp.229-242.

Liu, Y., Wang, M., Chen, T., Chiang, P., Huang, P. and Lee, J. (2006). Arsenate Sorption on Lithium/Aluminum Layered Double Hydroxide Intercalated by Chloride and on Gibbsite: Sorption Isotherms, Envelopes, and Spectroscopic Studies. *Environmental Science & Technology*, 40(24), pp.7784-7789.

Loganathan, S., Tikmani, M., Edubilli, S., Mishra, A. and Ghoshal, A. (2014). CO_2 adsorption kinetics on mesoporous silica under wide range of pressure and temperature. *Chemical Engineering Journal*, 256, pp.1-8.

Long, Y., Yu, J., Jiao, F. and Yang, W. (2016). Preparation and characterization of MWCNTs/LDHs nanohybrids for removal of Congo red from aqueous solution. *Transactions of Nonferrous Metals Society of China*, 26(10), pp.2701-2710.

Ma, L., Wang, Q., Islam, S., Liu, Y., Ma, S. and Kanatzidis, M. (2016). Highly Selective and Efficient Removal of Heavy Metals by Layered Double Hydroxide Intercalated with the MoS42–Ion. *Journal of the American Chemical Society*, 138(8), pp.2858-2866.

Mallakpour, S. and Hatami, M. (2017). Condensation polymer/layered double hydroxide NCs: Preparation, characterization, and utilizations. *European Polymer Journal*, 90, pp.273-300.

Matusinovic, Z. and Wilkie, C. (2012). Fire retardancy and morphology of layered double hydroxide nanocomposites: A review. *Journal of Materials Chemistry*, 22(36), pp.18701-18704

Mostafa, M., Bakr, A., El Naggar, A. and Sultan, E. (2016). Water decontamination via the removal of Pb (II) using a new generation of highly energetic surface nano-material: $Co^{2+}Mo^{6+}$ LDH. *Journal of Colloid and Interface Science*, 461, pp.261-272.

Mothe, G.K., Pakshirajan, K. and Das, G. (2017). Heavy metal removal from multicomponent system by sulfate reducing bacteria: mechanism and cell surface characterization. *Journal of Hazardous Materials*. 324, pp.62-70.

Namasivayam, C. and Sangeetha, D. (2008). Application of coconut coir pith for the removal of sulfate and other anions from water. *Desalination*. 219(1-3), pp.1-13

Ngulube, T., Gumbo, J., Masindi, V. and Maity, A. (2017). An update on synthetic dyes adsorption onto clay based minerals: A state-of-art review. Journal of Environmental Management, 191, pp.35-57.

Novillo, C., Guaya, D., Allen-Perkins Avendaño, A., Armijos, C., Cortina, J. and Cota, I. (2014). Evaluation of phosphate removal capacity of Mg/Al layered double hydroxides from aqueous solutions. *Fuel*, 138, pp.72-79.

Nurmi, B., Özkaya, B., Kasaki, K., Kaksonen, A.H., Riekola-Vanhanen, M., Tuovinen, O.H. and Puhakka, J.A. (2010). Biooxidation and precipitation for iron and sulfate removal from heap bioleaching effluent streams. Hydrometallurgy. 101. pp.7-14

Otgonjargal, E., Nyamsuren, B., Enkhtuul, S., Burmaa, G., Temuujin, J. and Khasbaatar, D. (2017). Removal of chromium from aqueous solution by thermally treated mgal layered double hydroxides. *Heighpubs Journal of Civil and Environmental Engineering*. 1. pp. 001-008.

Patist, A. and Bates, D. (2008). Ultrasonic innovations in the food industry: From the laboratory to commercial production. *Innovative Food Science & Emerging Technologies*, 9(2), pp.147-154.

Qian, J., Lu, H., Jiang, F., Ekama, G.A. and Chen, G-H. (2015). Beneficial co-treatment of simple wet flue gas desulphurization wastes with freshwater sewage through development of mixed denitrification-SANI process. *Chemical Engineering Journal*. 262, pp.109-118

Qiu, H., Lv, L., Pan, B., Zhang, Q., Zhang, W. and Zhang, Q. (2009). Critical review in adsorption kinetic models. *Journal of Zhejiang University-SCIENCE A*, 10(5), pp.716-724.

Qiu, L., Shi, L., Liu, Z., Xie, K., Wang, J., Zhang, S., Song, Q. and Lu, L. (2017). Effect of power ultrasound on crystallization characteristics of magnesium ammonium phosphate. *UltrasonicsSonochemistry*, 36, pp.123-128.

Qiu, X. and Wang, W. (2017). Removal of borate by layered double hydroxides prepared through microwave-hydrothermal method. *Journal of Water Process Engineering*, 17, pp.271-276.

Repo, E. (2011). *EDTA- and DTPA-Functionalized Silica Gel and Chitosan Adsorbents for the Removal of Heavy Metals from Aqueous Solutions*. Ph.D. Lappeenranta University of Technology.

Rodrigues, L. and da Silva, M. (2009). An investigation of phosphate adsorption from aqueous solution onto hydrous niobium oxide prepared by co-precipitation method. *Colloids and Surfaces A: Physicochemical and Engineering Aspects*, 334(1-3), pp.191-196.

Rojas, R. (2014). Copper, lead and cadmium removal by Ca/Al layered double hydroxides. *Applied Clay Science*, 87, pp.254-259.

Runtti, H., Luukkonen, T., Niskanen, M., Tuomikoski, S., Kangas, T., Tynjälä, P., Tolonen, E., Sarkkinen, M., Kemppainen, K., Rämö, J. and Lassi, U. (2016). Sulphate removal over barium-modified blast-furnace-slag geopolymer. *Journal of Hazardous Materials*, 317, pp.373-384.

Runtti, H., Tynjälä, P., Tuomikoski, S., Kangas, T., Hu, T., Rämö, J. and Lassi, U. (2017). Utilisation of barium-modified analcime in sulphate removal: Isotherms, kinetics and thermodynamics studies. *Journal of Water Process Engineering*, 16, pp.319-328.

Sadeghalvad, B., Azadmehr, A. and Hezarkhani, A. (2016). Enhancing adsorptive removal of sulfate by metal layered double hydroxide functionalized Quartz-Albitophire iron ore waste: preparation, characterization and properties. *RSC Adv.*, 6(72), pp.67630-67642.

Sadik, R., Lahkale, R., Hssaine, N., ElHatimi, W., Diouri, M., and Sabbar, E. (2015). Sulfate removal from wastewater by mixed oxide-LDH: Equilibrium, kinetic and thermodynamic studies. *Journal of Material Environment and Science*, 6(10), pp.2895-2905

Sajid, M. and Basheer, C. (2016). Layered double hydroxides: Emerging sorbent materials for analytical extractions. *TrAC Trends in Analytical Chemistry*, 75, pp.174-182.

Sepehr, M., Yetilmezsoy, K., Marofi, S., Zarrabi, M., Ghaffari, H., Fingas, M. and Foroughi, M. (2014). Synthesis of nanosheet layered double hydroxides at lower pH: Optimization of hardness and sulfate removal from drinking water samples. *Journal of the Taiwan Institute of Chemical Engineers*, 45(5), pp.2786-2800.

Shan, D., Cosnier, S. and Mousty, C. (2003). Layered Double Hydroxides: An Attractive Material for Electrochemical Biosensor Design. *Analytical Chemistry*, 75(15), pp.3872-3879.

Sharma, P. and Das, M. (2013). Removal of a Cationic Dye from Aqueous Solution Using Graphene Oxide Nanosheets: Investigation of Adsorption Parameters. *Journal of Chemical & Engineering Data*, 58(1), pp.151-158.

Silva, A.M., Lima, R. and Leao, V.A. (2012). Mine water treatment with limestone for sulfate removal. *Journal of Hazardous Materials*. (221), pp. 45-55.

Silva, R., Cadorin, L. and Rubio, J. (2010). Sulphate ions removal from an aqueous solution: I. Co-precipitation with hydrolyzed aluminum-bearing salts. Mineral Engineering. 23. pp.1220-1226

Tait, S., Clarke, W.P., Keller, J. and Batsonme, D.J. (2009). Removal of sulfate from high-strength wastewater by crystallization. Water Research. 43(3), pp.762-772.

Tang, S., Chia, G. and Lee, H. (2015). Magnetic core–shell iron(II,III) oxide@layered double oxide microspheres for removal of 2,5-dihydroxybenzoic acid from aqueous solutions. *Journal of Colloid and Interface Science*, 437, pp.316-323.

Theiss, F. (2012). *Synthesis and Characterization of Layered Double Hydroxides and Their Application for Water Purification*. Master of Applied Sciences. Queensland University of Technology.

Theiss, F., Ayoko, G. and Frost, R. (2016). Iodide removal using LDH technology. *Chemical Engineering Journal*, 296, pp.300-309.

Theiss, F.L., Ayoko, G.A. and Frost, R.L (2016). Synthesis of layered double hydroxides containing Mg^{2+}, Zn^{2+}, Ca^{2+} and Al^{3+} layer cations by co-precipitation methods – A review. *Applied Surface Science*, 383, pp.200-213.

Tichit, D. and Coq, B. (2003). Catalysis by Hydrotalcites and Related Materials. *CATTECH*, 7(6), pp.206-217.

Tillotson, S. (2006). Phosphate removal: an alternative to chemical dosing. *Filtration & Separation*, 43(5), pp.10-12.

Vaccari, A. (1998). Preparation and catalytic properties of cationic and anionic clays. *Catalysis Today*, 41(1-3), pp.53-71.

Van der Bruggen, B. and Vandecasteele, C. (2003). Removal of pollutants from surface water and groundwater by nanofiltration: overview of possible applications in the drinking water industry. *Environmental Pollution.* 122, pp. 435-445

Wan, S., Wang, S., Li, Y. and Gao, B. (2016). Functionalizing biochar with Mg–Al and Mg–Fe layered double hydroxides for removal of phosphate from aqueous solutions. *Journal of Industrial and Engineering Chemistry*. 47, pp.246-253.

Worch, E. (2012). *Adsorption technology in water treatment*. 1st ed. Berlin: Walter de Gruyter.

Yang, R. (2003). *Adsorbents*. 1st ed. Hoboken, N.J.: Wiley-Interscience.

Yang, K., Yan, L., Yang, Y., Y, S., Shan, R., Yu, H., Zhu, B. and Du, B. (2014). Adsorptive removal of phosphate by Mg-Al and Zn-Al layered double hydroxides: kinetics, isotherm and mechanism. *Separation and Purification Technology*. 124, pp.36-42

Yang, L., Shahrivari, Z., Liu, P., Sahimi, M. and Tsotsis, T. (2005). Removal of Trace Levels of Arsenic and Selenium from Aqueous Solutions by Calcined and Uncalcined Layered Double Hydroxides (LDH). *Industrial & Engineering Chemistry Research*, 44(17), pp.6804-6815.

Yu, Q., Zheng, Y., Wang, Y., Shen, L., Wang, H., Zheng, Y., He, N. and Li, Q. (2015). Highly selective adsorption of phosphate by pyromellitic acid intercalated ZnAl-LDHs: Assembling hydrogen bond acceptor sites. *Chemical Engineering Journal*, 260, pp.809-817.

Zhan, T., Zhang, Y., Yang, Q., Deng, H., Xu, J. and Hou, W. (2016). Ultrathin layered double hydroxide nanosheets prepared from a water-in-ionic liquid surfactant-free microemulsion for phosphate removal from aquatic systems. *Chemical Engineering Journal*, 302, pp.459-465.

Zhang, B., Luan, L., Gao, R., Li, F., Li, Y. and Wu, T. (2017). Rapid and effective removal of Cr(VI) from aqueous solution using exfoliated LDH nanosheets. *Colloids and Surfaces A: Physicochemical and Engineering Aspects*, 520, pp.399-408.

Zhou, J., Yang, S., Yu, J. and Shu, Z. (2011). Novel hollow microspheres of hierarchical zinc–aluminum layered double hydroxides and their enhanced adsorption capacity for phosphate in water. *Journal of Hazardous Materials*, 192(3), pp.1114-1121.

Zubair, M., Daud, M., McKay, G., Shehzad, F. and Al-Harthi, M. (2017). Recent progress in layered double hydroxides (LDH)-containing hybrids as adsorbents for water remediation. *Applied Clay Science*, 143, pp.279-292.

APPENDICES

APPENDIX 1. Patterns of the synthesized Zn-Al/LDH where cobalt cathode was used